MECHANICAL FOUR-POLE PARAMETERS: TRANSMISSION MATRICES

PENNSYLVANIA STATE UNIVERSITY
UNIVERSITY PARK, PENNSYLVANIA

19 APRIL 1976

MECHANICAL FOUR-POLE PARAMETERS: TRANSMISSION MATRICES

J. C. Snowdon

Technical Memorandum
File No. TM 76-122
April 19, 1976
Contract No. N00017-73-C-1418

Copy No. 57

The Pennsylvania State University
Institute for Science and Engineering
APPLIED RESEARCH LABORATORY
P. O. Box 30
State College, PA 16801

NAVY DEPARTMENT

NAVAL SEA SYSTEMS COMMAND

This investigation was sponsored by the Naval Sea Systems Command, Ship Silencing Division and the Office of Naval Research.

UNCLASSIFIED

SECURITY CLASSIFICATION OF THIS PAGE (When Data Entered)

REPORT DOCUMENTATION PAGE		READ INSTRUCTIONS BEFORE COMPLETING FORM
1. REPORT NUMBER TM 76-122	2. GOVT ACCESSION NO.	3. RECIPIENT'S CATALOG NUMBER
4. TITLE (and Subtitle) MECHANICAL FOUR-POLE PARAMETERS: TRANSMISSION MATRICES (U)		5. TYPE OF REPORT & PERIOD COVERED 6. PERFORMING ORG. REPORT NUMBER
7. AUTHOR(s) J. C. Snowdon		8. CONTRACT OR GRANT NUMBER(s) N00017-73-C-1418
9. PERFORMING ORGANIZATION NAME AND ADDRESS The Pennsylvania State University Applied Research Laboratory P. O. Box 30, State College, PA 16801		10. PROGRAM ELEMENT, PROJECT, TASK AREA & WORK UNIT NUMBERS SF 43-452-702 (Nav Sea) N00014-76-RQ-00002(ONR)
11. CONTROLLING OFFICE NAME AND ADDRESS Naval Sea Systems Command Department of the Navy Washington, DC 20362 Office of Naval Research Department of the Navy Arlington, VA 22217		12. REPORT DATE April 19, 1976 13. NUMBER OF PAGES 92
14. MONITORING AGENCY NAME & ADDRESS(if different from Controlling Office)		15. SECURITY CLASS. (of this report) UNCLASSIFIED 15a. DECLASSIFICATION/DOWNGRADING SCHEDULE

16. DISTRIBUTION STATEMENT (of this Report)

Approved for public release; distribution unlimited. Per NAVSEA Nov. 22, 1976

17. DISTRIBUTION STATEMENT (of the abstract entered in Block 20, if different from Report)

18. SUPPLEMENTARY NOTES

19. KEY WORDS (Continue on reverse side if necessary and identify by block number)

Four-pole parameters.
Transmission matrices.
Nonuniform beams.
Mass-loaded beams.
Circular plates.
Dynamic vibration absorbers.

20. ABSTRACT (Continue on reverse side if necessary and identify by block number)

This report revises and extends an earlier report entitled "Mechanical Four-Pole Parameters and their Application" [Journal of Sound and Vibration, 15, 307-323 (1971)]. Newly considered are so-called transmission matrices, which enable the transverse vibration response of beams with discontinuities to be analyzed readily. Further, the transmission matrices used in the report result in more concise beam analyses than the matrices generally employed in the literature. Additional examples that are

DD FORM 1 JAN 73 1473 EDITION OF 1 NOV 65 IS OBSOLETE

UNCLASSIFIED

SECURITY CLASSIFICATION OF THIS PAGE (When Data Entered)

considered here include end-driven cantilever beams or stanchions that are propped by a damped spring; or that carry an end mass having a finite moment of inertia; or that carry a mass that divides the stanchion into two stages of arbitrary lengths and cross-sectional areas; or that carry an end mass and subsequently comprise three stages having arbitrary lengths and cross-sectional areas.

ABSTRACT

This report revises and extends an earlier report entitled "Mechanical Four-Pole Parameters and their Application" (Journal of Sound and Vibration, 15, 307-323, 1970). Newly considered are so-called transmission matrices, which enable the transverse vibration response of beams with discontinuities to be analyzed readily. Further, the transmission matrices used in the report result in more concise beam analyses than the matrices generally employed in the literature. Additional examples that are considered here include end-driven cantilever beams or stanchions that are propped by a damped spring; or that carry an end mass having a finite moment of inertia; or that carry a mass that divides the stanchion into two stages of arbitrary lengths and cross-sectional areas; or that carry an end mass and subsequently comprise three stages having arbitrary lengths and cross-sectional areas.

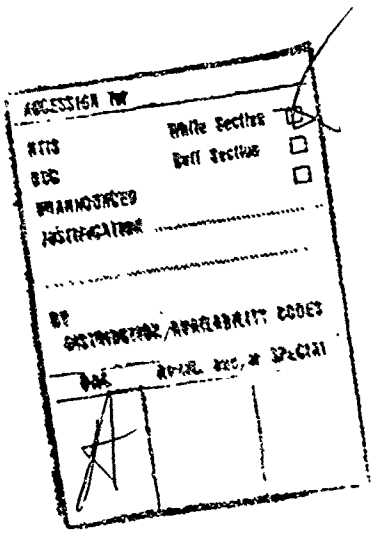

1. INTRODUCTION

Four-pole parameters have been utilized for many years in electrical circuit theory as an effective means of analyzing four-terminal networks[1-6]; more recently, with mechanical notation, they have been used to solve vibration problems involving rotational[7] and translational[8-14] motion. The four-pole parameters of a variety of mechanical elements that can be viewed as four-terminal devices are described here; for example, four-pole parameters are derived or stated for simple lumped systems such as a spring, a mass, and a dynamic vibration absorber, and for distributed systems such as a uniform rod in longitudinal vibration. Also stated are the parameters that describe the bending vibrations of a Bernoulli-Euler beam and a thin circular plate, both of which may be envisioned as four-terminal systems if they are driven and terminated so that only symmetrical vibrations about their midpoints are excited.

Four-pole parameter theory is actually a simple theory of transmission matrices. When more complicated situations are encountered than those mentioned hitherto, four-pole theory becomes inadequate and a transmission-matrix theory of wider applicability must be utilized.[15-23] For example, if a beam is not terminated symmetrically (as a cantilever), or is not driven symmetrically (as a simply supported beam driven off-center), it must be viewed as an eight-terminal system, and reliance must be placed on 4 x 4 transmission matrices rather than on the 2 x 2 matrices that typify the simpler four-pole theory.

Following a discussion of relevant four-pole parameters, and examples of their application, the more general transmission-matrix theory is developed and used, for example, to determine the transmissibility across a mass-loaded cantilever beam that comprises three sections of arbitrary lengths and cross-sectional areas, and across a cantilever beam that is mass loaded at an

arbitrary point marked also by a change in beam cross section. Although such problems are cumbersome to analyze conventionally, they are readily tractable using transmission-matrix theory.

2. BASIC FOUR-POLE THEORY

A linear mechanical system is shown schematically in Fig. 1. The system may be comprised of one or more lumped or distributed elements, or be constructed from any combination of such elements. The input side of the system vibrates simusoidally with a velocity $\tilde{V}_1$ in response to an applied force $\tilde{F}_1$. In turn, the output side of the system exerts a force $\tilde{F}_2$ on the input side of some further system, sharing with it a common velocity $\tilde{V}_2$. Thus, the system shown is said to have input and output terminal pairs, a force $\tilde{F}_1$ and velocity $\tilde{V}_1$ at the input terminal pair giving rise to a force $\tilde{F}_2$ and velocity $\tilde{V}_2$ at the output terminal pair, the reaction of any subsequent mechanical system being accounted for. Forces are considered positive when directed to the right.

Consider now the simusoidal vibration of a mass M and a spring K in the context of the foregoing discussion. From Newton's second law or Hooke's law, and from reference to Fig. 2(a) or 2(b), it is possible to write

1. Mass M

$$\tilde{F}_1 - \tilde{F}_2 = M \frac{d\tilde{V}_1}{dt} = M \frac{d\tilde{V}_2}{dt}$$

or

$$\tilde{F}_1 = \tilde{F}_2 + j\omega M \tilde{V}_2 \qquad (1)$$

and

$$\tilde{V}_1 = \tilde{V}_2 \ , \qquad (2)$$

where t is time and ω is angular frequency.

2. Spring K

$$\tilde{F}_1 = \tilde{F}_2 = K \int (\tilde{V}_1 - \tilde{V}_2)\, dt$$

or

$$\tilde{F}_1 = \tilde{F}_2 \tag{3}$$

and

$$\tilde{V}_1 = \tilde{F}_2 \left(\frac{j\omega}{K}\right) + \tilde{V}_2 \ . \tag{4}$$

Inspection of Eqs. 1-4 suggests that the vibration response of the four-terminal system of Fig. 1 can be represented by the following equations:

$$\tilde{F}_1 = \alpha_{11} \tilde{F}_2 + \alpha_{12} \tilde{V}_2 \tag{5}$$

and

$$\tilde{V}_1 = \alpha_{21} \tilde{F}_2 + \alpha_{22} \tilde{V}_2 \ , \tag{6}$$

where α_{11}, α_{12}, α_{21}, and α_{22} are known as four-pole parameters. It is directly apparent that

$$\alpha_{11} = \left.\frac{\tilde{F}_1}{\tilde{F}_2}\right|_{\tilde{V}_2=0} \ , \tag{7}$$

$$\alpha_{12} = \left.\frac{\tilde{F}_1}{\tilde{V}_2}\right|_{\tilde{F}_2=0} \ , \tag{8}$$

$$\alpha_{21} = \left.\frac{\tilde{V}_1}{\tilde{F}_2}\right|_{\tilde{V}_2=0} \ , \tag{9}$$

and

$$\alpha_{22} = \left.\frac{\tilde{V}_1}{\tilde{V}_2}\right|_{\tilde{F}_2=0} \ , \tag{10}$$

where the subscript $\tilde{V}_2 = 0$ indicates that the output terminal pair is blocked and the subscript $\tilde{F}_2 = 0$ indicates that the output terminal pair is free (unrestrained). The parameters α_{11} and α_{22} are dimensionless; α_{12} has the dimensions of impedance and α_{21} the dimensions of mobility.

In general, the four-pole parameters are frequency-dependent complex quantities. Of considerable advantage is the fact that the parameters characterize only the system for which they are determined; their value is not influenced by the preceeding or subsequent mechanical systems.

Equations 5 and 6 enable expressions for the driving-point and transfer impedances and for the force and displacement transmissibilities across the system to be written down concisely. Thus,

driving-point impedance,

$$Z_1 = \frac{\tilde{F}_1}{\tilde{V}_1} = \left(\frac{\alpha_{11}\,\tilde{F}_2 + \alpha_{12}\,\tilde{V}_2}{\alpha_{21}\,\tilde{F}_2 + \alpha_{22}\tilde{V}_2}\right) = \left(\frac{\alpha_{11}\,Z_T + \alpha_{12}}{\alpha_{21}\,Z_T + \alpha_{22}}\right) ; \tag{11}$$

transfer impedance,

$$TZ_{12} = \frac{\tilde{F}_1}{\tilde{V}_2} = (\alpha_{11}\,Z_T + \alpha_{12}) ; \tag{12}$$

force transmissibility,

$$T_{F12} = \left|\frac{\tilde{F}_2}{\tilde{F}_1}\right| = \left|\frac{Z_T}{(\alpha_{12} + \alpha_{11}\,Z_T)}\right| ; \tag{13}$$

and displacement transmissibility,

$$T_{D12} = \left|\frac{\tilde{V}_2}{\tilde{V}_1}\right| = \left|\frac{1}{(\alpha_{22} + \alpha_{21}\,Z_T)}\right| . \tag{14}$$

In these equations, $Z_T = \tilde{F}_2/\tilde{V}_2$ is the driving-point impedance of the mechanical system subsequent to the one under consideration.

3. RECIPROCITY AND TRANSMISSIBILITY THEOREMS

It is now instructive to return to the four-pole Eqs. 5 and 6, which are easily inverted to yield the equations

$$\tilde{F}_2 = \frac{\alpha_{22}}{\Delta} \tilde{F}_1 - \frac{\alpha_{12}}{\Delta} \tilde{V}_1 \tag{15}$$

and

$$\tilde{V}_2 = \frac{-\alpha_{21}}{\Delta} \tilde{F}_1 + \frac{\alpha_{11}}{\Delta} \tilde{V}_1 , \tag{16}$$

where

$$\Delta = (\alpha_{11}\, \alpha_{22} - \alpha_{12}\, \alpha_{21}) . \tag{17}$$

If the original output terminals are now visualized as the input terminal pair, the relevant four-pole equations follow immediately from Eqs. 15 and 16 in which the direction and, therefore, the sign of the forces $\tilde{F}_1$ and $\tilde{F}_2$ are reversed; thus,

$$\tilde{F}_2 = \frac{\alpha_{22}}{\Delta} \tilde{F}_1 + \frac{\alpha_{12}}{\Delta} \tilde{V}_1 \tag{18}$$

and

$$\tilde{V}_2 = \frac{\alpha_{21}}{\Delta} \tilde{F}_1 + \frac{\alpha_{11}}{\Delta} \tilde{V}_1 . \tag{19}$$

The Reciprocity Theorem states that the transfer impedance or mobility between any two terminal pairs in a network is independent of which terminal pair is taken as the input or output station; consequently,

$$\left.\frac{\tilde{F}_1}{\tilde{V}_2}\right|_{\tilde{F}_2=0} = \left.\frac{\tilde{F}_2}{\tilde{V}_1}\right|_{\tilde{F}_1=0} \tag{20}$$

or

$$\left.\frac{\tilde{V}_1}{\tilde{F}_2}\right|_{\tilde{V}_2=0} = \left.\frac{\tilde{V}_2}{\tilde{F}_1}\right|_{\tilde{V}_1=0} . \tag{21}$$

From either equation, reference to Eqs. 5 and 18, or Eqs. 6 and 19, shows that

$$\Delta = (\alpha_{11}\,\alpha_{22} - \alpha_{12}\,\alpha_{21}) = 1 \quad . \tag{22}$$

Consequently, Eqs. 18 and 19 may finally be written as

$$\tilde{F}_2 = \alpha_{22}\,\tilde{F}_1 + \alpha_{12}\,\tilde{V}_1 \tag{23}$$

and

$$\tilde{V}_2 = \alpha_{21}\,\tilde{F}_1 + \alpha_{11}\,\tilde{V}_1 \quad . \tag{24}$$

It follows from Eq. 22 that knowledge of only three of the four-pole parameters is sufficient to specify the performance of the system completely. Further, in the special case of a symmetrical system (when it does not matter which terminal pair is input or output), Eqs. 23 and 24 must be identical to Eqs. 5 and 6. That is to say, for a symmetrical system,

$$\alpha_{11} = \alpha_{22} \tag{25}$$

and knowledge of only two independent four-pole parameters is sufficient to determine the system performance completely.

Finally, an important result, which is sometimes referred to as the Transmissibility Theorem, follows immediately from Eqs. 5 and 24; thus,

$$\left.\frac{\tilde{F}_2}{\tilde{F}_1}\right|_{\tilde{V}_2=0} = \frac{1}{\alpha_{11}} = \left.\frac{\tilde{V}_1}{\tilde{V}_2}\right|_{\tilde{F}_1=0} \tag{26}$$

or transmissibility T is such that

$$T_{F12} = T_{D21} \quad . \tag{27}$$

Again, from Eqs. 6 and 23,

$$\left.\frac{\tilde{V}_2}{\tilde{V}_1}\right|_{\tilde{F}_2=0} = \frac{1}{\alpha_{22}} = \left.\frac{\tilde{F}_1}{\tilde{F}_2}\right|_{\tilde{V}_1=0} \tag{28}$$

or

$$T_{D12} = T_{F21} \quad . \tag{29}$$

Equations 27 and 29 show, as has frequently been noted and utilized in the past, that the force and displacement (and, therefore, velocity and acceleration) transmissibilities in opposite directions between the two terminal pairs of a mechanical system are identical.[24-27]

4. CONNECTION OF MECHANICAL FOUR-POLE SYSTEMS

If the output terminal pair of one mechanical system is rigidly connected to the input terminal pair of another system (Fig. 3), so that the output from

the first is exactly the input to the second, the two systems are connected in series. Thus, in matrix notation, if

$$\begin{bmatrix} \tilde{F}_1 \\ \tilde{V}_1 \end{bmatrix} = \begin{bmatrix} \alpha'_{11} & \alpha'_{12} \\ \alpha'_{21} & \alpha'_{22} \end{bmatrix} \begin{bmatrix} \tilde{F}_2 \\ \tilde{V}_2 \end{bmatrix} , \tag{30}$$

$$\begin{bmatrix} \tilde{F}_2 \\ \tilde{V}_2 \end{bmatrix} = \begin{bmatrix} \alpha''_{11} & \alpha''_{12} \\ \alpha''_{21} & \alpha''_{22} \end{bmatrix} \begin{bmatrix} \tilde{F}_3 \\ \tilde{V}_3 \end{bmatrix} , \tag{31}$$

and

$$\begin{bmatrix} \tilde{F}_n \\ \tilde{V}_n \end{bmatrix} = \begin{bmatrix} \alpha^{n}_{11} & \alpha^{n}_{12} \\ \alpha^{n}_{21} & \alpha^{n}_{22} \end{bmatrix} \begin{bmatrix} \tilde{F}_{(n+1)} \\ \tilde{V}_{(n+1)} \end{bmatrix} , \tag{32}$$

then

$$\begin{bmatrix} \tilde{F}_1 \\ \tilde{V}_1 \end{bmatrix} = \left\{ \begin{bmatrix} \alpha'_{11} & \alpha'_{12} \\ \alpha'_{21} & \alpha'_{22} \end{bmatrix} \begin{bmatrix} \alpha''_{11} & \alpha''_{12} \\ \alpha''_{21} & \alpha''_{22} \end{bmatrix} \cdots \begin{bmatrix} \alpha^{n}_{11} & \alpha^{n}_{12} \\ \alpha^{n}_{21} & \alpha^{n}_{22} \end{bmatrix} \right\} \begin{bmatrix} \tilde{F}_{(n+1)} \\ \tilde{V}_{(n+1)} \end{bmatrix} . \tag{33}$$

For a two-stage system,

$$\begin{bmatrix} \tilde{F}_1 \\ \tilde{V}_1 \end{bmatrix} = \begin{bmatrix} \beta_{11} & \beta_{12} \\ \beta_{21} & \beta_{22} \end{bmatrix} \begin{bmatrix} \tilde{F}_3 \\ \tilde{V}_3 \end{bmatrix} , \tag{34}$$

where

$$\begin{bmatrix} \beta_{11} & \beta_{12} \\ \beta_{21} & \beta_{22} \end{bmatrix} = \begin{bmatrix} \alpha'_{11}\alpha''_{11} + \alpha'_{12}\alpha''_{21} & \alpha'_{11}\alpha''_{12} + \alpha'_{12}\alpha''_{22} \\ \alpha'_{21}\alpha''_{11} + \alpha'_{22}\alpha''_{21} & \alpha'_{21}\alpha''_{12} + \alpha'_{22}\alpha''_{22} \end{bmatrix} . \tag{35}$$

If the input terminal pairs of two or more mechanical systems are connected rigidly so that they move with the same velocity (Fig. 4), and

if the net input and output forces are equal to the sum of the input and output forces of the component systems, then these systems are connected in parallel. Thus,

$$\begin{bmatrix} \tilde{F}_1 \\ \tilde{V}_1 \end{bmatrix} = \begin{bmatrix} \beta_{11} & \beta_{12} \\ \beta_{21} & \beta_{22} \end{bmatrix} \begin{bmatrix} \tilde{F}_2 \\ \tilde{V}_2 \end{bmatrix} , \tag{36}$$

where

$$\beta_{11} = A/B , \tag{37}$$

$$\beta_{12} = (AC - B^2)/B , \tag{38}$$

$$\beta_{21} = 1/B , \tag{39}$$

and

$$\beta_{22} = C/B . \tag{40}$$

In these equations,

$$A = \sum_{i=1}^{n} \left(\frac{\alpha_{11}^{i}}{\alpha_{21}^{i}} \right) , \tag{41}$$

$$B = \sum_{i=1}^{n} \left(\frac{1}{\alpha_{21}^{i}} \right) , \tag{42}$$

and

$$C = \sum_{i=1}^{n} \left(\frac{\alpha_{22}^{i}}{\alpha_{21}^{i}} \right) . \tag{43}$$

For only two systems in parallel,

$$A = \left(\frac{\alpha'_{11}\alpha''_{21} + \alpha'_{21}\alpha''_{11}}{\alpha'_{21}\alpha''_{21}}\right) = \frac{\varphi}{\epsilon} \quad , \tag{44}$$

$$B = \left(\frac{\alpha'_{21} + \alpha''_{21}}{\alpha'_{21}\alpha''_{21}}\right) = \frac{\vartheta}{\epsilon} \quad , \tag{45}$$

and

$$C = \left(\frac{\alpha'_{22}\alpha''_{21} + \alpha''_{22}\alpha'_{21}}{\alpha'_{21}\alpha''_{21}}\right) = \frac{\lambda}{\epsilon} \quad , \tag{46}$$

so that

$$\beta_{11} = \varphi/\vartheta \quad , \tag{47}$$

$$\beta_{12} = \beta_{22}\,(\varphi/\epsilon) - (\vartheta/\epsilon) \quad , \tag{48}$$

$$\beta_{21} = \epsilon/\vartheta \quad , \tag{49}$$

and

$$\beta_{22} = \lambda/\vartheta \quad . \tag{50}$$

5. VALUES OF FOUR-POLE PARAMETERS (LUMPED SYSTEMS)

1. Mass M [Fig. 2(a)]

Equations 1 and 2 show that, for this symmetrical system,

$$\alpha_{11} = \alpha_{22} = 1 \quad , \tag{51}$$

$$\alpha_{12} = j\omega M \quad , \tag{52}$$

$$\alpha_{21} = 0 \quad , \tag{53}$$

and

$$\begin{bmatrix} \tilde{F}_1 \\ \tilde{V}_1 \end{bmatrix} = \begin{bmatrix} 1 & j\omega M \\ 0 & 1 \end{bmatrix} \begin{bmatrix} \tilde{F}_2 \\ \tilde{V}_2 \end{bmatrix} . \tag{54}$$

2. Spring of Stiffness K [Fig. 2(b)]

Equations 3 and 4 show that

$$\alpha_{11} = \alpha_{22} = 1 , \tag{55}$$

$$\alpha_{12} = 0 , \tag{56}$$

$$\alpha_{21} = j\omega/K , \tag{57}$$

and

$$\begin{bmatrix} \tilde{F}_1 \\ \tilde{V}_1 \end{bmatrix} = \begin{bmatrix} 1 & 0 \\ \frac{j\omega}{K} & 1 \end{bmatrix} \begin{bmatrix} \tilde{F}_2 \\ \tilde{V}_2 \end{bmatrix} . \tag{58}$$

Equally well, for a rubberlike material having a complex modulus G^*_ω, K would simply be replaced by the complex stiffness kG^*_ω, where k is an appropriate constant having the dimensions of length.[27]

3. Dashpot of Viscosity η (Fig. 5)

$$\tilde{F}_1 = \tilde{F}_2 \tag{59}$$

and

$$\tilde{V}_1 = \tilde{F}_2/\eta + \tilde{V}_2 . \tag{60}$$

Consequently,

$$\alpha_{11} = \alpha_{22} = 1 \,, \tag{61}$$

$$\alpha_{12} = 0 \,, \tag{62}$$

$$\alpha_{21} = 1/\eta \,, \tag{63}$$

and

$$\begin{bmatrix} \tilde{F}_1 \\ \tilde{V}_1 \end{bmatrix} = \begin{bmatrix} 1 & 0 \\ 1/\eta & 1 \end{bmatrix} \begin{bmatrix} \tilde{F}_2 \\ \tilde{V}_2 \end{bmatrix} \,. \tag{64}$$

4. Parallel Spring and Dashpot (Fig. 6)

$$\tilde{F}_1 = \tilde{F}_2 \tag{65}$$

and

$$\tilde{V}_1 = \kappa^* \tilde{F}_2 + \tilde{V}_2 \,, \tag{66}$$

where

$$\kappa^* = \left(\frac{K}{j\omega} + \eta \right)^{-1} \,. \tag{67}$$

Consequently,

$$\alpha_{11} = \alpha_{22} = 1 \,, \tag{68}$$

$$\alpha_{12} = 0 \,, \tag{69}$$

$$\alpha_{21} = \kappa^* \,, \tag{70}$$

and

$$\begin{bmatrix} \tilde{F}_1 \\ \tilde{V}_1 \end{bmatrix} = \begin{bmatrix} 1 & 0 \\ \kappa^* & 1 \end{bmatrix} \begin{bmatrix} \tilde{F}_2 \\ \tilde{V}_2 \end{bmatrix} = \begin{bmatrix} 1 & 0 \\ \dfrac{j\omega}{K[1+(j\omega\eta/K)]} & 1 \end{bmatrix} \begin{bmatrix} \tilde{F}_2 \\ \tilde{V}_2 \end{bmatrix} . \tag{71}$$

This equation shows that the parallel spring and dashpot combination may be regarded as a single spring of complex stiffness $K^* = K[1 + (j\omega\eta/K)]$.

5. Dynamic Absorber (Fig. 7)

It follows directly that

$$\begin{bmatrix} \tilde{F}_1 \\ \tilde{V}_1 \end{bmatrix} = \begin{bmatrix} 1 & 0 \\ \kappa^* & 1 \end{bmatrix} \begin{bmatrix} 1 & j\omega M \\ 0 & 1 \end{bmatrix} \begin{bmatrix} \tilde{F}_3 \\ \tilde{V}_3 \end{bmatrix}$$

$$= \begin{bmatrix} 1 & j\omega M \\ \kappa^* & 1+j\omega M\kappa^* \end{bmatrix} \begin{bmatrix} \tilde{F}_3 \\ \tilde{V}_3 \end{bmatrix} . \tag{72}$$

A dynamic absorber is normally unterminated ($Z_T = \tilde{F}_3/\tilde{V}_3$ equals zero), in which case its driving-point impedance Z_a may be written simply as

$$Z_a = \frac{\tilde{F}_1}{\tilde{V}_1} = \frac{j\omega M}{(1 + j\omega M\kappa^*)} . \tag{73}$$

6. Mechanical System with Dynamic Absorber (Fig. 8)

As before, let

$$\begin{bmatrix} \tilde{F}_2 \\ \tilde{V}_2 \end{bmatrix} = \begin{bmatrix} \alpha_{11} & \alpha_{12} \\ \alpha_{21} & \alpha_{22} \end{bmatrix} \begin{bmatrix} \tilde{F}_3 \\ \tilde{V}_3 \end{bmatrix} . \tag{74}$$

If the driving-point impedance of the dynamic absorber is again Z_a, then

$$\tilde{F}_1 = \tilde{F}_2 + Z_a \tilde{V}_2 \tag{75}$$

and, since $\tilde{V}_1 = \tilde{V}_2$, it is possible to write

$$\begin{bmatrix} \tilde{F}_1 \\ \tilde{V}_1 \end{bmatrix} = \begin{bmatrix} 1 & Z_a \\ 0 & 1 \end{bmatrix} \begin{bmatrix} \tilde{F}_2 \\ \tilde{V}_2 \end{bmatrix} . \tag{76}$$

It simply follows that

$$\begin{bmatrix} \tilde{F}_1 \\ \tilde{V}_1 \end{bmatrix} = \begin{bmatrix} 1 & Z_a \\ 0 & 1 \end{bmatrix} \begin{bmatrix} \alpha_{11} & \alpha_{12} \\ \alpha_{21} & \alpha_{22} \end{bmatrix} \begin{bmatrix} \tilde{F}_3 \\ \tilde{V}_3 \end{bmatrix} \tag{77}$$

or

$$\begin{bmatrix} \tilde{F}_1 \\ \tilde{V}_1 \end{bmatrix} = \begin{bmatrix} \alpha_{11}+Z_a\alpha_{21} & \alpha_{12}+Z_a\alpha_{22} \\ \alpha_{21} & \alpha_{22} \end{bmatrix} \begin{bmatrix} \tilde{F}_3 \\ \tilde{V}_3 \end{bmatrix} , \tag{78}$$

where Z_a is given by Eq. (73).

6. VALUES OF FOUR-POLE PARAMETERS (DISTRIBUTED SYSTEMS WITH INTERNAL DAMPING)

6.1 Uniform Thin Rod

For the longitudinal vibration of this symmetrical system,[27] which is shown in Fig. 9,

$$\alpha_{11} = \frac{\tilde{F}_1}{\tilde{F}_2}\bigg|_{\tilde{V}_2=0} = \cos n^*\ell = \alpha_{22} \ , \tag{79}$$

$$\alpha_{12} = \frac{\tilde{F}_1}{\tilde{V}_2}\bigg|_{\tilde{F}_2=0} = \mu_R^* \sin n^*\ell \ , \tag{80}$$

and

$$\alpha_{21} = \frac{(\alpha_{11}\alpha_{22}-1)}{\alpha_{12}} = \frac{(-\sin^2 n^*\ell)}{\mu_R^* \sin n^*\ell} = \frac{-\sin n^*\ell}{\mu_R^*} \ , \tag{81}$$

where

$$\mu_R^* = (j\omega M_R/n^*\ell) \ , \tag{82}$$

and ℓ and M_R are the length and mass of the rod; n^* is the complex wavenumber.[27]

Knowledge of the four-pole parameters enables expressions for the impedance and force and displacement transmissibilities of the rod to be written down directly from reference to Eqs. 11-14. The termination impedance in these equations can have any value. When $Z_T = 0$ or ∞, results for the limiting case of a free-free rod or a free-clamped rod can be obtained. If the rod is connected to other lumped or distributed systems, equations equivalent to Eqs. 11-14 will describe the vibration response of the resultant system.

For example, the force transmissibility T_{F12} across a rod loaded by a mass M at its driven end, and terminated rigidly at its opposite end, follows directly from inspection of Eq. 13; that is to say,

$$T_{F12} = |\beta_{11}|^{-1} , \tag{83}$$

where

$$\begin{bmatrix} \beta_{11} & \beta_{12} \\ \beta_{21} & \beta_{22} \end{bmatrix} = \begin{bmatrix} 1 & j\omega M \\ 0 & 1 \end{bmatrix} \begin{bmatrix} \cos n^*\ell & \mu_R^* \sin n^*\ell \\ (-1/\mu_R^*)\sin n^*\ell & \cos n^*\ell \end{bmatrix} . \tag{84}$$

Consequently,

$$T_{F12} = |[\cos n^*\ell - (M/M_R)(n^*\ell)\sin n^*\ell]|^{-1} . \tag{85}$$

This equation has been used, as in Ref. 27, to provide a guide to the character of so-called "wave-effects" in antivibration mountings, where the force-driven mass M and the rod are visualized as a vibrating machine and a resilient mount, which has self resonances by virtue of its elasticity and finite mass M_R.

6.2 Bernoulli-Euler Beam

In general, transversely vibrating beams must be viewed as eight-terminal systems, since the application of rotational as well as translational forces and velocities must be accounted for. However, in the restricted but important case where the beams are excited in <u>symmetrical</u> vibration by sinusoidal forces, they may be visualized as four-pole networks if their output forces can be shared between dual output terminals. Then, for a center-driven beam (Fig. 10), two sets of four-pole parameters relate to the two pairs of boundary conditions that are most frequently considered in practice. Thus, if it is assumed that the bending moment is

always zero at the ends of the beam, the adoption of blocked or free terminal pairs will provide the limiting cases of a simply supported or a free-free beam. Alternatively, if it is assumed that the ends of the beam are constrained to have zero slope, the adoption of blocked or free terminal pairs will provide the limiting cases of a clamped-clamped beam or a beam with ends free to slide without restraint (zero shearing force). In either case, it must be assumed that half the driving-point impedance Z_T of the subsequent mechanical system can be placed at each end of the beam: Eqs. 11-14 then remain directly applicable.

(1) Zero Bending Moment at Ends of Beam

Reference to the expressions for beam impedance and transmissibility in Chaps. 7 and 9 of Ref. 27 shows that the relevant four-pole parameters are

$$\alpha_{11} = \left(\frac{2\ \text{ch.c.}}{\text{ch.+c.}}\right)_{(n^*a)} , \tag{86}$$

$$\alpha_{12} = \mu_b^* \left(\frac{\text{sh.c.+ch.s.}}{\text{ch.+c.}}\right)_{(n^*a)} , \tag{87}$$

$$\alpha_{21} = \frac{1}{\mu_b^*} \left(\frac{\text{sh.c.-ch.s}}{\text{ch.+c.}}\right)_{(n^*a)} , \tag{88}$$

and

$$\alpha_{22} = \left(\frac{\text{ch.c.+1}}{\text{ch.+c.}}\right)_{(n^*a)} , \tag{89}$$

where

$$\mu_b^* = (j\omega M_b/n^*a) ; \tag{90}$$

M_b and a are the mass and the half-length of the beam, and n^* is its complex wavenumber.[27] Abbreviations such as $(\text{ch.c.})_{(n^*a)}$, for example, are used

to represent the term cosh n^*a cos n^*a. Although the beam responds as a symmetrical system in the following discussion, it has not done so here because $\alpha_{11} \neq \alpha_{22}$ (Eq. 25).

(2) Zero Slope at Ends of Beam

The four-pole parameters now become

$$\alpha_{11} = \alpha_{22} = \left(\frac{\text{sh.c.+ch.s.}}{\text{sh.+s.}}\right)_{(n^*a)} , \tag{91}$$

$$\alpha_{12} = \mu_b^* \left(\frac{2\ \text{sh.s.}}{\text{sh.+s.}}\right)_{(n^*a)} , \tag{92}$$

and

$$\alpha_{21} = \frac{1}{\mu_b^*} \left(\frac{\text{ch.c.-1}}{\text{sh.+s.}}\right)_{(n^*a)} . \tag{93}$$

(3) Examples

Knowledge of the foregoing four-pole parameters and of the results of Eqs. 11-14 enables expressions for beam impedance and transmissibility to be written down directly. For example, reference to Eqs. 11 and 91-93 shows that the driving-point impedance Z_m of a beam centrally loaded by a mass M, and rigidly clamped at each end, can be written as

$$Z_m = \frac{\beta_{11}}{\beta_{21}} , \tag{94}$$

where

$$\begin{bmatrix} \beta_{11} & \beta_{12} \\ \beta_{21} & \beta_{22} \end{bmatrix} = \frac{1}{(\text{sh.+s.})_{(n^*a)}} \begin{bmatrix} 1 & j\omega M \\ 0 & 1 \end{bmatrix} \begin{bmatrix} (\text{sh.c.+ch.s.}) & 2\mu_b^*(\text{sh.s.}) \\ (\mu_b^*)^{-1}(\text{ch.c.-1}) & (\text{sh.c.+ch.s.}) \end{bmatrix}_{(n^*a)} ; \tag{95}$$

consequently,

$$\frac{Z_m}{j\omega M_b} = \left[\frac{(sh.c.+ch.s.) + (M/M_b)(n^*a)(ch.c.-1)}{n^*a(ch.c.-1)} \right]_{(n^*a)} . \tag{96}$$

Likewise, from Eqs. 11 and 86-89, the driving-point impedance Z_{om} of a free-free beam, the ends of which are loaded equally by lumped masses M having negligible rotary inertia. is given by the equation

$$Z_{om} = \frac{\beta_{12}}{\beta_{22}} , \tag{97}$$

where

$$\begin{bmatrix} \beta_{11} & \beta_{12} \\ \beta_{21} & \beta_{22} \end{bmatrix} = \frac{1}{(ch.+c.)_{(n^*a)}} \begin{bmatrix} 2(ch.c.) & \mu_b^*(sh.c.+ch.s.) \\ (\mu_b^*)^{-1}(sh.c.-ch.s.) & (ch.c.+1) \end{bmatrix}_{(n^*a)} \begin{bmatrix} 1 & 2j\omega M \\ 0 & 1 \end{bmatrix} ; \tag{98}$$

consequently

$$\frac{Z_{om}}{j\omega M_b} = \frac{1}{(n^*a)} \left[\frac{(sh.c.+ch.s.) + 4\ (M/M_b)(n^*a)(ch.c.)}{(ch.c.+1) + 2\ (M/M_b)(n^*a)(sh.c.-ch.s.)} \right]_{(n^*a)} . \tag{99}$$

Note that, because the beam is loaded by a total mass 2M, a corresponding impedance of $2j\omega M$ appears in the final matrix of Eq. 98.

Finally, the force transmissibility $T_{F12} = T_m$ across a simply supported beam that is centrally loaded by a mass M can be written from Eqs. 13 and 86-89 as follows:

$$T_m = |\beta_{11}|^{-1} , \tag{100}$$

where now

$$\begin{bmatrix} \beta_{11} & \beta_{12} \\ \beta_{21} & \beta_{22} \end{bmatrix} = \frac{1}{(\text{ch.}+\text{c.})(n^*a)} \begin{bmatrix} 1 & j\alpha M \\ 0 & 1 \end{bmatrix} \begin{bmatrix} 2(\text{ch.c.}) & \mu_b^*(\text{sh.c.}+\text{ch.s.}) \\ (\mu_b^*)^{-1}(\text{sh.c.}-\text{ch.s.}) & (\text{ch.c.}+1) \end{bmatrix}_{(n^*a)} ; \quad (101)$$

consequently,

$$T_m = \left| \frac{(\text{ch.}+\text{c.})}{2(\text{ch.c.}) + (M/M_b)(n^*a)(\text{sh.c.}-\text{ch.s.})} \right|_{(n^*a)} . \quad (102)$$

6.3 Thin Circular Plate

The transverse vibration of a thin circular plate excited symmetrically by a simusoidally varying force (Ref. 28) can also be predicted by the use of four-pole parameters. Such a plate of mass M_p and radius r = a is shown in Fig. 11. The plate is driven by a central point force $\tilde{F}_1$ that gives rise to a force $\tilde{F}_2$ per unit arc length at the plate boundary. Associated with these forces are the velocities $\tilde{V}_1$ and $\tilde{V}_2$.

In common with the beams considered in the foregoing, two sets of four-pole parameters relate to the two pairs of limiting plate boundary conditions most frequently encountered in practice:

(1) Zero Bending Moment at Plate Boundary

In this case, the extreme values of $Z_T = (2\pi a\, \tilde{F}_2/\tilde{V}_2) = 0$ or ∞ in Eqs. 11-14 provide results for a plate with a free or a simply supported boundary. The four-pole parameters of the plate are

$$\alpha_{11} = \Xi^*/\Omega^* , \quad (103)$$

$$\alpha_{12} = 2\mu_p^*\, \Theta^*/\Omega^* , \quad (104)$$

$$\alpha_{21} = (n^*a)\, \Psi^*/4\Lambda\mu_p^*\Omega^* , \quad (105)$$

and

$$\alpha_{22} = (n^*a)\,\Phi^*/2\Lambda\Omega^* \,, \tag{106}$$

where

$$\Lambda = 2/\pi \,, \tag{107}$$

$$\mu_p^* = j\omega M_p/(n^*a) \,, \tag{108}$$

$$\Xi^* = [-2J_oI_o + \phi_a^*(J_oI_1 + J_1I_o)]_{(n^*a)} \,, \tag{109}$$

$$\Omega^* = [-(J_o + I_o) + \phi_a^*(J_1 + I_1)]_{(n^*a)} \,, \tag{110}$$

$$\Theta^* = [-(J_oI_1 + J_1I_o) + 2\phi_a^*J_1I_1]_{(n^*a)} \,, \tag{111}$$

$$\Phi^* = \{[(J_o+I_o)(Y_1-\Lambda K_1)-(J_1-I_1)(Y_o-\Lambda K_o)] - 2\phi_a^*(Y_1I_1-\Lambda J_1K_1)\}_{(n^*a)} \,, \tag{112}$$

and

$$\Psi^* = \{2(Y_oI_o + \Lambda J_oK_o) + \phi_a^*[(J_o-I_o)(Y_1+\Lambda K_1)-(J_1+I_1)(Y_o+\Lambda K_o)]\}_{(n^*a)} \,. \tag{113}$$

In these equations, n^* is the complex wavenumber of the plate,[28] abbreviations such as $(J_oI_1)_{(n^*a)}$ refer to the product $J_o(n^*a)I_1(n^*a)$ of the ordinary and modified Bessel Functions of orders zero and one having the complex argument (n^*a), and

$$\phi_a^* = (1 - \nu^*)/(n^*a) \,, \tag{114}$$

where ν^* is the complex Poisson's ratio of the plate material.[28]

(2) Zero Slope at Plate Boundary

In this case, the extreme values of $Z_T = 0$ or ∞ in Eqs. 11-14 provide results for a plate with a sliding or a rigidly clamped boundary, and

$$\alpha_{11} = \left(\frac{J_o I_1 + J_1 I_o}{J_1 + I_1}\right)_{(n^*a)} , \tag{115}$$

$$\alpha_{12} = 4\mu_p^* \left(\frac{J_1 I_1}{J_1 + I_1}\right)_{(n^*a)} , \tag{116}$$

$$\alpha_{21} = \left(\frac{n^*a}{4\Lambda\mu_p^*}\right) \frac{x^*}{(J_1 + I_1)_{(n^*a)}} , \tag{117}$$

and

$$\alpha_{22} = \left(\frac{n^*a}{\Lambda}\right)\left(\frac{\Lambda J_1 K_1 - Y_1 I_1}{J_1 + I_1}\right)_{(n^*a)} , \tag{118}$$

where

$$x^* = [(J_o - I_o)(Y_1 + \Lambda K_1) - (J_1 + I_1)(Y_o + \Lambda K_o)]_{(n^*a)} . \tag{119}$$

(3) Examples

As an example, if in Case (1) the terminating impedance Z_T at the plate boundary is not specified, reference to Eqs. 13, 103, and 104 shows that the force transmissibility $T_{F12} = T_{FO}$ across the plate is simply

$$T_{FO} = \left|\frac{2\pi a \tilde{F}_2}{\tilde{F}_1}\right| = \left|\frac{[(n^*a)\, Z_T/j\omega M_p]\, \Omega^*}{\{2\Theta^* + [(n^*a)\, Z_T/j\omega M_p]\, \Xi^*\}}\right| . \tag{120}$$

This equation states that, if the boundary of the plate is completely free, $T_{FO} = 0$; alternatively, if it is simply (rigidly) supported,

$$T_{FO} = |\Omega^*/\Xi^*| . \tag{121}$$

Likewise, in Case (2), if the boundary of the plate is built-in (clamped), and if a dynamic absorber is attached to the plate where it is driven by

the central force $\tilde{F}_1$, then the transmissibility T_{Fa} across the plate follows directly from reference to Eqs. 78, 115, and 117:

$$T_{Fa} = |2\pi a \tilde{F}_2/\tilde{F}_1| = |(\alpha_{11} + Z_a \alpha_{21})|^{-1}$$

$$= \left| \left[\frac{8(J_1 + I_1)}{8(J_o I_1 + J_1 I_o) + \pi(n*a)^2 x*(Z_a/j\omega M_p)} \right] \right|_{(n*a)} , \qquad (122)$$

where the driving-point impedance Z_a of the dynamic absorber is given by Eq. 73.

The use of a dynamic absorber to reduce the vibration of platelike structures is discussed in Refs. 14 and 29-33. Because of the practical importance of the dynamic absorber in such applications, transmissibility curves that have been computed from Eq. 122 are plotted and described in the following section.

7. DYNAMIC ABSORBER ATTACHED TO A CIRCULAR PLATE CLAMPED AT ITS BOUNDARY

Calculations of the transmissibility T_{Fa} can be made from Eq. 122 more conveniently if the impedance of the dynamic absorber is written from Eq. 73 as

$$Z_a = \frac{j\omega M_a [1 + j(\omega\eta_a/K_a)]}{[1 - (\omega/\omega_a)^2 + j(\omega\eta_a/K_a)]} . \qquad (123)$$

Here, the subscript a relates K, M, and η specifically to the absorber, which has the natural frequency

$$\omega_a = (K_a/M_a)^{\frac{1}{2}} . \qquad (124)$$

The dimensionless quantity $(\omega\eta_a/K_a)$ can be expressed in terms of a frequency ratio (ω_a/ω_m) and a damping ratio

$$\delta_R = \frac{\eta_a}{2M_a\omega_a} = \frac{\eta_a}{\eta_{ac}} \quad ; \tag{125}$$

this is explained in detail in Ref. 27, which considers the attachment of dynamic absorbers to cantilever beams. In the present applications, ω_m is the frequency of the fundamental plate resonance to which the absorber is tuned; η_{ac} is the value of the coefficient of viscosity required to damp the absorber critically; and the frequency ω is related to the plate wave number[28] by the equation

$$\frac{\omega}{\omega_m} = \left(\frac{na}{N}\right)^2 , \tag{126}$$

where N = 3.1962 is the value taken by na at the fundamental resonant frequency ω_m when the internal damping of the plate is negligible.

Optimum design of the dynamic absorber is achieved, for any given value of M_a, by suitable choice of values for the frequency or tuning ratio ω_a/ω_m and the damping ratio δ_R. For these so-called optimum values, which will be written as $(\omega_a/\omega_m)_o$ and $(\delta_R)_o$, the transmissibility T_{Fa} at the fundamental plate resonance is suppressed in a uniform and symmetrical manner. The optimum values are chosen here in exactly the same way as is described in Ref. 27. Results obtained for several values of the mass ratio M_a/M_p appear in Table I together with the resultant values of the maximum transmissibility $(T_{Fa})_{max}$ across the plate at its fundamental resonance. In each case, the plate damping factors are equal to 0.01,

and the tabulated values of $(T_{Fa})_{max}$ may be compared with the large maximum value of transmissibility $T_F \approx 170$ observed when no absorber is attached to the plate.

Representative calculations of T_{Fa} for the two heaviest absorber masses considered here are plotted in Fig. 12 as a function of the dimensionless quantity na, which is proportional to the square root of frequency. The dashed-line curve shows the transmissibility across the plate in the absence of the dynamic absorber. As observed for the cantilever beam in Ref. 27, not only is the absorber effective in suppressing the resonance to which it is tuned, but its relatively large damping is also effective in suppressing the plate resonances at higher frequencies. Thus, the displacement of the absorber mass decreases rapidly at frequencies above ω_a, so that the mass becomes a "fixed" point from which the absorber dashpot is able to restrain the motion of the plate at resonance.

Should the plate be simply supported rather than clamped around its boundary, $N \approx 2.2325$ and the optimum values of (ω_a/ω_m) and δ_R become those listed in Table II. Although these values differ from those of Table I, the resultant levels of maximum transmissibility change only by approximately 15%.

8. VALUES OF TRANSMISSION MATRICES (LUMPED SYSTEMS)

As explained in the Introduction, transversely vibrating beams are properly regarded as eight-terminal systems because, in general, it is necessary to account not only for their translational velocity response $\tilde{V}$ but also for their rotational velocity response $\tilde{\theta}$ to an impressed force $\tilde{F}$ and/or bending moment $\tilde{B}$. The simple transmission matrices of the lumped elements of mass and stiffness considered hitherto can readily be extended to an eight-terminal format. Because this extension is primarily to facilitate analyses of combined beam-lumped element systems, the new matrices are developed according to the sign convention utilized previously in beam analyses.[27] Thus, at the left-hand end of a beam positioned along the x axis, force is positive downward and bending moment is anticlockwise positive; at the right-hand end of the beam, force is positive upward and bending moment is clockwise positive; translational displacement $\tilde{y}$ is always positive upward; and rotational displacement $\partial\tilde{y}/\partial x$ is always positive anticlockwise.

1. Mass M [Fig. 13(a)]

If the mass has a negligible moment of inertia, it is possible to state that

$$\tilde{F}_1 = \tilde{F}_2 - j\omega M\tilde{V}_2 \quad , \tag{127}$$

$$\tilde{V}_1 = \tilde{V}_2 \quad , \tag{128}$$

$$\tilde{B}_1 = \tilde{B}_2 \quad , \tag{129}$$

$$\tilde{\theta}_1 = \tilde{\theta}_2 \quad , \tag{130}$$

and

$$\begin{bmatrix} \tilde{F}_1 \\ \tilde{V}_1 \\ \tilde{B}_1 \\ \tilde{\theta}_1 \end{bmatrix} = \begin{bmatrix} 1 & -j\omega M & 0 & 0 \\ 0 & 1 & 0 & 0 \\ 0 & 0 & 1 & 0 \\ 0 & 0 & 0 & 1 \end{bmatrix} \begin{bmatrix} \tilde{F}_2 \\ \tilde{V}_2 \\ \tilde{B}_2 \\ \tilde{\theta}_2 \end{bmatrix} , \tag{131}$$

where $\tilde{V} = j\omega\tilde{y}$ and $\tilde{\theta} = j\omega\partial\tilde{y}/\partial x$.

2. Mass M Having a Finite Moment of Inertia I [Fig. 13(b)]

Equations 127, 128, and 130 remain relevant, but Eq. 129 now becomes

$$\tilde{B}_1 = \tilde{B}_2 + j\omega I\tilde{\theta}_2 \quad , \tag{132}$$

so that

$$\begin{bmatrix} \tilde{F}_1 \\ \tilde{V}_1 \\ \tilde{B}_1 \\ \tilde{\theta}_1 \end{bmatrix} = \begin{bmatrix} 1 & -j\omega M & 0 & 0 \\ 0 & 1 & 0 & 0 \\ 0 & 0 & 1 & j\omega I \\ 0 & 0 & 0 & 1 \end{bmatrix} \begin{bmatrix} \tilde{F}_2 \\ \tilde{V}_2 \\ \tilde{B}_2 \\ \tilde{\theta}_2 \end{bmatrix} . \tag{133}$$

3. Spring of Stiffness K in Cascade [Fig. 14(a)]

If the spring also possesses a rotational stiffness K_R,

$$\tilde{F}_1 = \tilde{F}_2 \quad , \tag{134}$$

$$\tilde{V}_1 = -(j\omega/K)\,\tilde{F}_2 + \tilde{V}_2 \quad , \tag{135}$$

$$\tilde{B}_1 = \tilde{B}_2 \quad , \tag{136}$$

and

$$\tilde{\theta}_1 = \tilde{\theta}_2 + (j\omega/K_R)\tilde{B}_2 \quad ; \tag{137}$$

however, if the rotational stiffness K_R is very large,

$$\tilde{\theta}_1 = \tilde{\theta}_2 \quad , \tag{138}$$

in which case

$$\begin{bmatrix} \tilde{F}_1 \\ \tilde{V}_1 \\ \tilde{B}_1 \\ \tilde{\theta}_1 \end{bmatrix} = \begin{bmatrix} 1 & 0 & 0 & 0 \\ -\frac{j\omega}{K} & 1 & 0 & 0 \\ 0 & 0 & 1 & 0 \\ 0 & 0 & 0 & 1 \end{bmatrix} \begin{bmatrix} \tilde{F}_2 \\ \tilde{V}_2 \\ \tilde{B}_2 \\ \tilde{\theta}_2 \end{bmatrix} \quad . \tag{139}$$

4. Supported Spring of Stiffness K [Fig. 14(b)]

If the spring now has negligible rotational stiffness, Eqs. 136 and 138 remain relevant and Eqs. 134 and 135 become

$$\tilde{F}_1 = \tilde{F}_2 - (K/j\omega)\tilde{V}_2 \tag{140}$$

and

$$\tilde{V}_1 = \tilde{V}_2 \quad ; \tag{141}$$

consequently,

$$\begin{bmatrix} \tilde{F}_1 \\ \tilde{V}_1 \\ \tilde{B}_1 \\ \tilde{\theta}_1 \end{bmatrix} = \begin{bmatrix} 1 & -\frac{K}{j\omega} & 0 & 0 \\ 0 & 1 & 0 & 0 \\ 0 & 0 & 1 & 0 \\ 0 & 0 & 0 & 1 \end{bmatrix} \begin{bmatrix} \tilde{F}_2 \\ \tilde{V}_2 \\ \tilde{B}_2 \\ \tilde{\theta}_2 \end{bmatrix} \quad . \tag{142}$$

5. Dashpot of Viscosity η [Fig. 14(c)]

Equations 134 and 136 remain applicable, Eq. 138 is also applicable if the dashpot has very large rotational viscosity, and $(1/\eta)$ replaces $(j\omega/K)$ in Eq. 135; thus,

$$\begin{bmatrix} \tilde{F}_1 \\ \tilde{V}_1 \\ \tilde{B}_1 \\ \tilde{\theta}_1 \end{bmatrix} = \begin{bmatrix} 1 & 0 & 0 & 0 \\ -\frac{1}{\eta} & 1 & 0 & 0 \\ 0 & 0 & 1 & 0 \\ 0 & 0 & 0 & 1 \end{bmatrix} \begin{bmatrix} \tilde{F}_2 \\ \tilde{V}_2 \\ \tilde{B}_2 \\ \tilde{\theta}_2 \end{bmatrix} \quad . \tag{143}$$

6. Parallel Spring and Dashpot

The appropriate transmission matrix is readily seen to be that of Eq. 139 in which the element $-(j\omega/K)$ has been replaced by $-\kappa^*$, where κ^* is defined by Eq. 67.

7. Dynamic Absorber

If the translational driving-point impedance of the (unterminated) dynamic absorber is Z_a, as in Eq. 123, the appropriate transmission matrix is that of Eq. 131 in which the element $-j\omega M$ has been replaced by $-Z_a$.

9. VALUES OF TRANSMISSION MATRICES (BERNOULLI-EULER BEAMS WITH INTERNAL DAMPING)

The expressions given in Ref. 27 for transverse beam displacement and its successive time derivatives make it possible to state that

$$\tilde{F} = j\omega n^* \epsilon^* \left(P^* \sinh n^* x + Q^* \sin n^* x + R^* \cosh n^* x - S^* \cos n^* x\right) e^{j\omega t} \quad , \tag{144}$$

$$\tilde{V} = j\omega \left(P^* \cosh n^* x + Q^* \cos n^* x + R^* \sinh n^* x + S^* \sin n^* x\right) e^{j\omega t} \quad , \tag{145}$$

$$\tilde{B} = j\omega \epsilon^* \left(P^* \cosh n^* x - Q^* \cos n^* x + R^* \sinh n^* x - S^* \sin n^* x\right) e^{j\omega t} \quad , \tag{146}$$

and

$$\tilde{\theta} = j\omega n^* \left(P^* \sinh n^* x - Q^* \sin n^* x + R^* \cosh n^* x + S^* \cos n^* x\right) e^{j\omega t} \quad ; \qquad (147)$$

in these equations, P^*, Q^*, R^*, and S^* are arbitrary complex constants and

$$\epsilon^* = -\frac{E^* I (n^*)^2}{j\omega} \quad , \qquad (148)$$

where n^* is the complex beam wavenumber, I is the second moment of area of the beam cross section, and E^* is the complex Young's modulus of the beam material. Equations 144 - 147 can readily be expressed in matrix form as

$$\begin{bmatrix} \tilde{F} \\ \tilde{V} \\ \tilde{B} \\ \tilde{\theta} \end{bmatrix} = j\omega \begin{bmatrix} n^*\epsilon^* \sinh n^* x & n^*\epsilon^* \sin n^* x & n^*\epsilon^* \cosh n^* x & -n^*\epsilon^* \cos n^* x \\ \cosh n^* x & \cos n^* x & \sinh n^* x & \sin n^* x \\ \epsilon^* \cosh n^* x & -\epsilon^* \cos n^* x & \epsilon^* \sinh n^* x & -\epsilon^* \sin n^* x \\ n^* \sinh n^* x & -n^* \sin n^* x & n^* \cosh n^* x & n^* \cos n^* x \end{bmatrix} \begin{bmatrix} P^* \\ Q^* \\ R^* \\ S^* \end{bmatrix} e^{j\omega t} \quad . \qquad (149)$$

Suppose, now, that $x = 0$ at the beam input terminals (location 1 in Fig. 15); then

$$\begin{bmatrix} \tilde{F}_1 \\ \tilde{V}_1 \\ \tilde{B}_1 \\ \tilde{\theta}_1 \end{bmatrix} = j\omega \begin{bmatrix} 0 & 0 & n^*\epsilon^* & -n^*\epsilon^* \\ 1 & 1 & 0 & 0 \\ \epsilon^* & -\epsilon^* & 0 & 0 \\ 0 & 0 & n^* & n^* \end{bmatrix} \begin{bmatrix} P^* \\ Q^* \\ R^* \\ S^* \end{bmatrix} e^{j\omega t} \quad . \qquad (150)$$

The square transmission matrix of this equation can be inverted in a straightforward way if the equation is considered to have the two components

$$\begin{bmatrix} \tilde{F}_1 \\ \tilde{\theta}_1 \end{bmatrix} = j\omega n^* \begin{bmatrix} \epsilon^* & -\epsilon^* \\ 1 & 1 \end{bmatrix} \begin{bmatrix} R^* \\ S^* \end{bmatrix} e^{j\omega t} \tag{151}$$

and

$$\begin{bmatrix} \tilde{V}_1 \\ \tilde{B}_1 \end{bmatrix} = j\omega \begin{bmatrix} 1 & 1 \\ \epsilon^* & -\epsilon^* \end{bmatrix} \begin{bmatrix} P^* \\ Q^* \end{bmatrix} e^{j\omega t} \quad , \tag{152}$$

for which it can be stated that

$$\begin{bmatrix} R^* \\ S^* \end{bmatrix} = \frac{e^{-j\omega t}}{2j\omega n^* \epsilon^*} \begin{bmatrix} 1 & \epsilon^* \\ -1 & \epsilon^* \end{bmatrix} \begin{bmatrix} \tilde{F}_1 \\ \tilde{\theta}_1 \end{bmatrix} \tag{153}$$

and

$$\begin{bmatrix} P^* \\ Q^* \end{bmatrix} = \frac{e^{-j\omega t}}{2j\omega \epsilon^*} \begin{bmatrix} \epsilon^* & 1 \\ \epsilon^* & -1 \end{bmatrix} \begin{bmatrix} \tilde{V}_1 \\ \tilde{B}_1 \end{bmatrix} \quad ; \tag{154}$$

consequently,

$$\begin{bmatrix} P^* \\ Q^* \\ R^* \\ S^* \end{bmatrix} = \frac{e^{-j\omega t}}{2j\omega} \begin{bmatrix} 0 & 1 & \frac{1}{\epsilon^*} & 0 \\ 0 & 1 & -\frac{1}{\epsilon^*} & 0 \\ \frac{1}{n^* \epsilon^*} & 0 & 0 & \frac{1}{n^*} \\ -\frac{1}{n^* \epsilon^*} & 0 & 0 & \frac{1}{n^*} \end{bmatrix} \begin{bmatrix} \tilde{F}_1 \\ \tilde{V}_1 \\ \tilde{B}_1 \\ \tilde{\theta}_1 \end{bmatrix} . \tag{155}$$

Again, suppose that $x = \ell$ at the beam output terminals (location 2 in Fig. 15); then, from Eq. 149,

$$\begin{bmatrix} \tilde{F}_2 \\ \tilde{V}_2 \\ \tilde{B}_2 \\ \tilde{\theta}_2 \end{bmatrix} = j\omega \begin{bmatrix} n^*\epsilon^* sh. & n^*\epsilon^* s. & n^*\epsilon^* ch. & -n^*\epsilon^* c. \\ ch. & c. & sh. & s. \\ \epsilon^* ch. & -\epsilon^* c. & \epsilon^* sh. & -\epsilon^* s. \\ n^* sh. & -n^* s. & n^* ch. & n^* c. \end{bmatrix}_{(n^*\ell)} \begin{bmatrix} P^* \\ Q^* \\ R^* \\ S^* \end{bmatrix} e^{j\omega t} , \tag{156}$$

where the abbreviations ch., c., sh., and s., are used to denote the quantities $\cosh n^*\ell$, $\cos n^*\ell$. $\sinh n^*\ell$, and $\sin n^*\ell$.

From reference to Eqs. 155 and 156 it is possible to state that

$$\{\Gamma_2\} = \tfrac{1}{2}\,[\Pi_1][\Pi_2]\{\Gamma_1\} = [\Pi_3]\{\Gamma_1\} , \tag{157}$$

where the column vectors

$$\{\Gamma_i\} = \begin{bmatrix} \tilde{F}_i \\ \tilde{V}_i \\ \tilde{B}_i \\ \tilde{\theta}_i \end{bmatrix} \qquad (i = 1,2) \tag{158}$$

and the matrices

$$[\Pi_1] = \begin{bmatrix} n^*\epsilon^* sh. & n^*\epsilon^* s. & n^*\epsilon^* ch. & -n^*\epsilon^* c. \\ ch. & c. & sh. & s. \\ \epsilon^* ch. & -\epsilon^* c. & \epsilon^* sh. & -\epsilon^* s. \\ n^* sh. & -n^* s. & n^* ch. & n^* c. \end{bmatrix}_{(n^*\ell)} , \tag{159}$$

$$[\Pi_2] = \begin{bmatrix} 0 & 1 & \frac{1}{\epsilon^*} & 0 \\ 0 & 1 & -\frac{1}{\epsilon^*} & 0 \\ \frac{1}{n^*\epsilon^*} & 0 & 0 & \frac{1}{n^*} \\ \frac{-1}{n^*\epsilon^*} & 0 & 0 & \frac{1}{n^*} \end{bmatrix} , \tag{160}$$

and

$$[\Pi_3] = \tfrac{1}{2} \begin{bmatrix} (ch.+c.) & n^*\epsilon^*(sh.+s.) & n^*(sh.-s.) & \epsilon^*(ch.-c.) \\ \frac{1}{n^*\epsilon^*}(sh.-s.) & (ch.+c.) & \frac{1}{\epsilon^*}(ch.-c.) & \frac{1}{n^*}(sh.+s.) \\ \frac{1}{n^*}(sh.+s.) & \epsilon^*(ch.-c.) & (ch.+c.) & \frac{\epsilon^*}{n^*}(sh.-s.) \\ \frac{1}{\epsilon^*}(ch.-c.) & n^*(sh.-s.) & \frac{n^*}{\epsilon^*}(sh.+s.) & (ch.+c.) \end{bmatrix}_{(n^*\ell)} . \tag{161}$$

Further,

$$\{\Gamma_1\} = [\Pi_3]^{-1}\{\Gamma_2\} = [\Pi]\{\Gamma_2\} , \tag{162}$$

where it can be verified that

$$[\Pi] = \tfrac{1}{2}\begin{bmatrix} (ch.+c.) & -n^*\epsilon^*(sh.+s.) & -n^*(sh.-s.) & \epsilon^*(ch.-c.) \\ \frac{-1}{n^*\epsilon^*}(sh.-s.) & (ch.+c.) & \frac{1}{\epsilon^*}(ch.-c.) & -\frac{1}{n^*}(sh.+s.) \\ -\frac{1}{n^*}(sh.+s.) & \epsilon^*(ch.-c.) & (ch.+c.) & -\frac{\epsilon^*}{n^*}(sh.-s.) \\ \frac{1}{\epsilon^*}(ch.-c.) & -n^*(sh.-s.) & -\frac{n^*}{\epsilon^*}(sh.+s.) & (ch.+c.) \end{bmatrix}_{(n^*\ell)} . \qquad (163)$$

An advantage exists to relating the state vectors at the input and output beam terminals 1 and 2 by the matrix Eq. 162 rather than by Eq. 157. Thus, apart from maintaining similarity with the matrix equations encountered in previous Sections, two of the elements of the column vector $\{\Gamma_2\}$ will always be zero for the simply supported, free, or clamped beam terminations that are usually discussed in the literature; conversely, in forced-vibration problems, only one or none of the elements of the column vector $\{\Gamma_1\}$ will be zero. Consequently, when a beam with several discontinuities has to be analyzed, and the overall transmission matrix incorporates the product of several component transmission matrices having the form of Eq. 163, there is no need to calculate three or all four columns of the overall matrix; rather, throughout, only two columns need to be calculated and algebraic complexity is minimized. Even the analysis of a uniform beam is facilitated to some extent. Thus, as a simple example, the bending-moment impedance BZ_o at the center of a beam [Fig. 16(a)] without discontinuities, and with simply supported terminations for which $\tilde{B}_2 = \tilde{V}_2 = 0$, can be determined as follows: One half of the applied bending moment $\tilde{B}_1$ is considered to act

on one half of the beam of length $a = \ell/2$, producing at the driving point an internal shearing force $\tilde{F}_1$ and a rotational velocity $\tilde{\theta}_1$. Equation 162 can then be written as

$$\begin{bmatrix} \tilde{F}_1 \\ 0 \\ \tilde{B}_1/2 \\ \tilde{\theta}_1 \end{bmatrix} = \frac{1}{2} \begin{bmatrix} (\text{ch.}+\text{c.}) & \cdot & \cdot & \epsilon^*(\text{ch.}-\text{c.}) \\ \frac{-1}{n^*\epsilon^*}(\text{sh.}-\text{s.}) & \cdot & \cdot & \frac{-1}{n^*}(\text{sh.}+\text{c.}) \\ -\frac{1}{n^*}(\text{sh.}+\text{s.}) & \cdot & \cdot & \frac{-\epsilon^*}{n^*}(\text{sh.}-\text{s.}) \\ \frac{1}{\epsilon^*}(\text{ch.}-\text{c.}) & \cdot & \cdot & (\text{ch.}+\text{c.}) \end{bmatrix}_{(n^*a)} \begin{bmatrix} \tilde{F}_2 \\ 0 \\ 0 \\ \tilde{\theta}_2 \end{bmatrix} , \quad (164)$$

where the hyperbolic and circular functions within the transmission matrix have been assigned the argument n^*a. It follows that

$$0 = -\frac{1}{n^*\epsilon^*}(\text{sh.}-\text{s.})_{(n^*a)} \tilde{F}_2 - \frac{1}{n^*}(\text{sh.}+\text{s.})_{(n^*a)} \tilde{\theta}_2 , \quad (165)$$

$$\tilde{B}_1 = -\frac{1}{n^*}(\text{sh.}+\text{s.})_{(n^*a)} \tilde{F}_2 - \frac{\epsilon^*}{n^*}(\text{sh.}-\text{s.})_{(n^*a)} \tilde{\theta}_2 , \quad (166)$$

and

$$\tilde{\theta}_1 = \frac{1}{2\epsilon^*}(\text{ch.}-\text{c.})_{(n^*a)} \tilde{F}_2 + \frac{1}{2}(\text{ch.}+\text{c.})_{(n^*a)} \tilde{\theta}_2 ; \quad (167)$$

therefore, if Eq. 165 is used to eliminate $\tilde{F}_2$ from Eqs. 166 and 167, and the ratio is taken of the resultant expressions for $\tilde{B}_1$ and $\tilde{\theta}_1$, the required moment impedance is

$$BZ_o = \frac{\tilde{B}_1}{\tilde{\theta}_1} = 4 \left(\frac{\text{sh.s.}}{\text{sh.c.-ch.s.}} \right)_{(n^* a)} \frac{\epsilon^*}{n^*} \quad . \tag{168}$$

This quantity is conveniently normalized by division by a moment impedance $j\omega I_b$--the impedance at the midpoint of an ideally rigid free beam of the same dimensions and mass M_b as the simply supported beam under consideration here; thus,

$$\frac{BZ_o}{j\omega I_b} = \frac{6}{(n^* a)^3} \left(\frac{\text{sh.s.}}{\text{sh.c.-ch.s.}} \right)_{(n^* a)} \quad , \tag{169}$$

where the moment of inertia $I_b = M_b a^2/3$.

To conclude this Section, it is instructive to note that, if a beam termination has the translational and rotational impedances $Z_T = \tilde{F}_2/\tilde{V}_2$ and $Z_R = -\tilde{B}_2/\tilde{\theta}_2$, the matrix Eq. 162 may be rephrased as follows:

$$\begin{bmatrix} \tilde{F}_1 \\ \tilde{V}_1 \\ \tilde{B}_1 \\ \tilde{\theta}_1 \end{bmatrix} = \frac{1}{2} \begin{bmatrix} \alpha_{11} & \alpha_{12} & \alpha_{13} & \alpha_{14} \\ \alpha_{21} & \alpha_{22} & \alpha_{23} & \alpha_{24} \\ \alpha_{31} & \alpha_{32} & \alpha_{33} & \alpha_{34} \\ \alpha_{41} & \alpha_{42} & \alpha_{43} & \alpha_{44} \end{bmatrix} \begin{bmatrix} \tilde{F}_2 \\ \tilde{F}_2/Z_T \\ \tilde{B}_2 \\ -\tilde{B}_2/Z_R \end{bmatrix} \quad , \tag{170}$$

where the complex parameters $\alpha_{11} = (\text{ch.+c.})_{(n^* \ell)}$, $\alpha_{32} = \epsilon^* (\text{ch.-c.})_{(n^* \ell)}$, $\alpha_{42} = -n^* (\text{sh.-s.})_{(n^* \ell)}$, etc.; the negative sign in the definition of Z_R arises because, at the beam termination, the positive directions of $\tilde{B}_2$ and $\tilde{\theta}_2$ are opposed (Fig. 15). It is readily seen that

$$\tilde{F}_1 = \frac{(\alpha_{11}Z_T + \alpha_{12})\tilde{F}_2}{2Z_T} + \frac{(\alpha_{13}Z_R - \alpha_{14})\tilde{B}_2}{2Z_R} \quad , \tag{171}$$

$$\tilde{V}_1 = \frac{(\alpha_{21}Z_T + \alpha_{22})\tilde{F}_2}{2Z_T} + \frac{(\alpha_{23}Z_R - \alpha_{24})\tilde{B}_2}{2Z_R} \quad , \tag{172}$$

and

$$\tilde{B}_1 = \frac{(\alpha_{31}Z_T + \alpha_{32})\tilde{F}_2}{2Z_T} + \frac{(\alpha_{33}Z_R - \alpha_{34})\tilde{B}_2}{2Z_R} \quad . \tag{173}$$

These cumbersome equations become tractable if either $\tilde{F}_1$ or $\tilde{B}_1$ is zero. For example, if $\tilde{B}_1 = 0$, as would be true if there were no applied bending moment at the free (input-terminal) end of a beam such as a cantilever or free-free beam, then it is possible to eliminate the parameter

$$\tilde{B}_2 = - \frac{Z_R}{Z_T} \left(\frac{\alpha_{31}Z_T + \alpha_{32}}{\alpha_{33}Z_R - \alpha_{34}} \right) \tilde{F}_2 \tag{174}$$

from Eqs. 171 and 172 to yield expressions for impedance and transmissibility that are analogous to those given initially (Eqs. 11-14) for a four-terminal system. Thus,

driving-point impedance,

$$Z_1 = \frac{\tilde{F}_1}{-\tilde{V}_1} = - \frac{\zeta^*}{\psi^*} \quad ; \tag{175}$$

transfer impedance,

$$TZ_{12} = \frac{\tilde{F}_1}{-\tilde{V}_2} = - \frac{\zeta^*}{\upsilon^*} \quad ; \tag{176}$$

force transmissibility,

$$T_{F12} = \left|\frac{\tilde{F}_2}{\tilde{F}_1}\right| = \left|\frac{Z_T \upsilon^*}{\zeta^*}\right| \quad ; \tag{177}$$

and displacement transmissibility,

$$T_{D12} = \left|\frac{\tilde{V}_2}{\tilde{V}_1}\right| = \left|\frac{\upsilon^*}{\psi^*}\right| \quad ; \tag{178}$$

again, the negative signs are introduced in the definitions of Z_1 and TZ_{12} because the positive direction of $\tilde{F}_1$ is opposed to that of the velocities $\tilde{V}_1$ and $\tilde{V}_2$. In the foregoing equations,

$$\zeta^* = [(\alpha_{31}Z_T + \alpha_{32})(\alpha_{13}Z_R - \alpha_{14}) - (\alpha_{11}Z_T + \alpha_{12})(\alpha_{33}Z_R - \alpha_{34})] \quad , \tag{179}$$

$$\psi^* = [(\alpha_{31}Z_T + \alpha_{32})(\alpha_{23}Z_R - \alpha_{24}) - (\alpha_{21}Z_T + \alpha_{22})(\alpha_{33}Z_R - \alpha_{34})] \quad , \tag{180}$$

and

$$\upsilon^* = -2\,(\alpha_{33}Z_R - \alpha_{34}) \quad . \tag{181}$$

For a clamped beam termination, $Z_T = Z_1 = \infty$ and, for example, the equations for driving-point impedance and force transmissibility simplify as follows:

$$Z_1 = \left(\frac{\alpha_{11}\alpha_{33} - \alpha_{31}\alpha_{13}}{\alpha_{31}\alpha_{23} - \alpha_{21}\alpha_{33}}\right) \tag{182}$$

and

$$T_{F12} = \left|\frac{2\alpha_{33}}{(\alpha_{11}\alpha_{33} - \alpha_{31}\alpha_{13})}\right| \quad . \tag{183}$$

Note that elements from only the first and third columns of the transmission matrix (Eq. 170) appear here. For a simply supported termination, $Z_T = \infty$ and $Z_R = 0$; consequently,

$$Z_1 = -\left(\frac{\alpha_{11}\alpha_{34} - \alpha_{31}\alpha_{14}}{\alpha_{21}\alpha_{34} - \alpha_{31}\alpha_{24}}\right) \tag{184}$$

and

$$T_{F12} = \left|\frac{2\alpha_{34}}{(\alpha_{11}\alpha_{34} - \alpha_{31}\alpha_{14})}\right| \quad . \tag{185}$$

In this case, elements from only the first and fourth columns of the transmission matrix are present. Finally, for a free termination, $Z_T = Z_R = 0$, $T_{F12} = 0$, and the relevant equation for driving-point impedance contains elements from only the second and fourth columns of the matrix.

10. CANTILEVER BEAMS HAVING VARIOUS CONFIGURATIONS

Several important cantilever-beam vibration problems that can be analyzed readily and concisely by transmission matrices are considered in this final Section. Three of the problems concern force-driven beams with clamped terminations for which Eqs. 182 and 183 remain directly applicable. Considered in a fourth problem is a beam driven by a force and a bending moment simultaneously.

10.1 Spring-Supported Cantilever Beam

Determined first, as a simple example, are the driving-point impedance and transmissibility of a force-driven beam that is supported by a spring of complex stiffness $K^* = K(1 + j\delta_K)$ at its free end, as in Fig. 16(b). Reference to Eqs. 142 and 163 shows that

$$\begin{bmatrix} \tilde{F}_1 \\ \tilde{V}_1 \\ 0 \\ \tilde{\theta}_1 \end{bmatrix} = \begin{bmatrix} 1 & \frac{-K^*}{j\omega} & 0 & 0 \\ 0 & 1 & 0 & 0 \\ 0 & 0 & 1 & 0 \\ 0 & 0 & 0 & 1 \end{bmatrix} \begin{bmatrix} (ch.+c.) & . & -n^*(sh.-s.) & . \\ -\frac{1}{n^*\epsilon^*}(sh.-s.) & . & \frac{1}{\epsilon^*}(ch.-c.) & . \\ -\frac{1}{n^*}(sh.+s.) & . & (ch.+c.) & . \\ \frac{1}{\epsilon^*}(ch.-c.) & . & \frac{-n^*}{\epsilon^*}(sh.+s.) & . \end{bmatrix} \begin{bmatrix} \tilde{F}_2 \\ 0 \\ \tilde{B}_2 \\ 0 \end{bmatrix} \tag{186}$$

and, consequently, that the overall transmission matrix possesses the elements

$$\alpha_{11} = \tfrac{1}{2}\,[(ch.+c.) + k^*(sh.-s.)]_{(n^*\ell)} \quad , \tag{187}$$

$$\alpha_{13} = \frac{-n^*}{2}\,[(sh.-s.) + k^*(ch.-c.)]_{(n^*\ell)} \quad , \tag{188}$$

$$\alpha_{21} = -\frac{1}{2n^*\epsilon^*}(sh.-s.)_{(n^*\ell)} \quad , \tag{189}$$

$$\alpha_{23} = \frac{1}{2\epsilon^*}(ch.-c.)_{(n^*\ell)} \quad , \tag{190}$$

$$\alpha_{31} = -\frac{1}{2n^*}(sh.+s.)_{(n^*\ell)} \quad , \tag{191}$$

and

$$\alpha_{33} = \tfrac{1}{2}\,(ch.+c.)_{(n^*\ell)} \quad . \tag{192}$$

It readily follows that

$$(\alpha_{11}\alpha_{33} - \alpha_{31}\alpha_{13}) = \tfrac{1}{2}\,[(ch.c.+1) + k^*(sh.c.-ch.s.)]_{(n^*\ell)} \quad , \tag{193}$$

$$(\alpha_{31}\alpha_{23} - \alpha_{21}\alpha_{33}) = \frac{1}{2n^{*}\epsilon^{*}} (\text{sh.c.}-\text{ch.s.})_{(n^{*}\ell)} \quad , \tag{194}$$

and, from inspection of Eqs. 182 and 183, that

$$\frac{Z_1}{j\omega M_b} = \left[\frac{(\text{ch.c.}+1) + k^{*}(\text{sh.c.}-\text{ch.s.})}{n^{*}\ell(\text{sh.c.}-\text{ch.s.})}\right]_{(n^{*}\ell)} \tag{195}$$

and

$$T_{F12} = \left|\frac{2(\text{ch.}+\text{c.})}{(\text{ch.c.}+1) + k^{*}(\text{sh.c.}-\text{ch.s.})}\right|_{(n^{*}\ell)} \quad . \tag{196}$$

In these equations,

$$k^{*} = \frac{K^{*}}{j\omega n^{*}\epsilon^{*}} = \frac{-3}{(n^{*}\ell)^3}\left(\frac{K}{K_T}\right)\left(\frac{1 + j\delta_K}{1 + j\delta_E}\right) \quad , \tag{197}$$

where δ_E is the beam damping factor and $K_T = 3EI/\ell^3$ is the static stiffness of an unsupported cantilever beam loaded transversely at its free end.

10.2 Cantilever Beam with a Tip Mass M Having a Finite Moment of Inertia I

In this example, the cantilever beam is driven simultaneously by a vibratory force $\tilde{F}_1$ and a bending moment $\tilde{B}_1$ at its free end, as in Fig. 16(c). Reference to Eqs. 133 and 163 shows that the resultant vibration response of the beam is governed by the equation

$$\begin{bmatrix} 1 \\ 1 \\ 1 \\ 1 \end{bmatrix} = \frac{1}{2} \begin{bmatrix} 1 & -j\alpha M & 0 & 0 \\ 0 & 1 & 0 & 0 \\ 0 & 0 & 1 & j\omega I \\ 0 & 0 & 0 & 1 \end{bmatrix} \begin{bmatrix} (ch.+c.) & . & -n^*(sh.-s.) & . \\ -\frac{1}{n^*\epsilon^*}(sh.-s.) & . & \frac{1}{\epsilon^*}(ch.-c.) & . \\ -\frac{1}{n^*}(sh.+s.) & . & (ch.+c.) & . \\ \frac{1}{\epsilon^*}(ch.-c.) & . & \frac{-n^*}{\epsilon^*}(sh.+s.) & . \end{bmatrix}_{(n^*\ell)} \begin{bmatrix} \tilde{F}_2 \\ 0 \\ \tilde{B}_2 \\ 0 \end{bmatrix}$$

$$= \frac{1}{2} \begin{bmatrix} [(ch.+c.) + \frac{j\alpha M}{n^*\epsilon^*}(sh.-s.)] & . & -n^*[(sh.-s.) + \frac{j\alpha M}{n^*\epsilon^*}(ch.-c.)] & . \\ \frac{-1}{n^*\epsilon^*}(sh.-s.) & . & \frac{1}{\epsilon^*}(ch.-c.) & . \\ \frac{-1}{n^*}[(sh.+s.) - \frac{j\omega I n^*}{\epsilon^*}(ch.-c.)] & . & [(ch.+c.) - \frac{j\omega I n^*}{\epsilon^*}(sh.+s.)] & . \\ \frac{1}{\epsilon^*}(ch.-c.) & . & -\frac{n^*}{\epsilon^*}(sh.+s.) & . \end{bmatrix}_{(n^*\ell)} \begin{bmatrix} \tilde{F}_2 \\ 0 \\ \tilde{B}_2 \\ 0 \end{bmatrix}, \tag{198}$$

where

$$\frac{j\alpha M}{n^*\epsilon^*} = \frac{M}{M_b}(n^*\ell) = \gamma(n^*\ell) \tag{199}$$

and

$$\frac{j\omega I n^*}{\epsilon^*} = \frac{I}{3I_b}(n^*\ell)^3 = \sigma(n^*\ell)^3 \quad . \tag{200}$$

(Recall here that $I_b = M_b\ell^2/3$ is the moment of inertia about the end of a rigid free beam having the same length, cross-sectional area A, and density

ρ as the cantilever beam under discussion; and that $(n^*)^4 = \omega^2\rho/r_g^2E^* = \omega^2\rho A/E^*I$, where r_g is the radius of gyration of the beam cross section.)

It is readily seen from Eq. 198 that

$$2\tilde{F}_1 = \tilde{F}_2[(ch.+c.) + \gamma(n^*\ell)(sh.-s.)]_{(n^*\ell)} - \tilde{B}_2 n^*[(sh.-s.) + \gamma(n^*\ell)(ch.-c.)]_{(n^*\ell)} \quad (201)$$

and

$$2\tilde{B}_1 = \frac{-\tilde{F}_2}{n^*}[(sh.+s.) - \sigma(n^*\ell)^3(ch.-c.)]_{(n^*\ell)} + \tilde{B}_2[(ch.+c.) - \sigma(n^*\ell)^3(sh.+s.)]_{(n^*\ell)} \quad . \quad (202)$$

Therefore, if $\tilde{B}_2$ or $\tilde{F}_2$ is eliminated from this pair of simultaneous equations, it is possible to write

$$12 = \left|\frac{\tilde{F}_2}{\tilde{F}_1}\right| = \left|\left\{[(ch.+c.) - \sigma(n^*\ell)^3(sh.+s.)] + (n^*\ell)f^*(\omega)[(sh.-s.) + \gamma(n^*\ell)(ch.-c.)]\right\}\xi^*\right|_{(n^*\ell)} \quad (203)$$

or

$$12 = \left|\frac{\tilde{B}_2}{\tilde{B}_1}\right| = \left|\left\{[(ch.+c.) + \gamma(n^*\ell)(sh.-s.)] + [(n^*\ell)f^*(\omega)]^{-1}[(sh.+s.) - \sigma(n^*\ell)^3(ch.-c.)]\right\}\xi^*\right|_{(n^*\ell)}, \quad (204)$$

where

$$\xi^* = [(ch.c.+1) + \gamma(n^*\ell)(sh.c.-ch.s.) - \sigma(n^*\ell)^3(sh.c.+ch.s.) - \gamma\sigma(n^*\ell)^4(ch.c.-1)]^{-1}_{(n^*\ell)} \quad (205)$$

and

$$\tilde{B}_1 = (\tilde{F}_1\ell)f^*(\omega) \quad . \quad (206)$$

The function of frequency $f^*(\omega)$ will be specified for each problem of concern, and it will be a real rather than a complex number if the applied force and bending moment are of like phase. Although a cantilever beam with a mass having finite moment of inertia has been considered in Refs. 34-37, attention was confined to the natural frequencies of the beam in free vibration; beam response to forced vibration was not considered, as it has been here.

Representative calculations of force transmissibility are plotted in Fig. 17 as a function of $n\ell$, a dimensionless quantity that is proportional to the square root of frequency. It has been assumed that $f(\omega) = 0.5$, $\gamma = M/M_b = 5$, $\sigma = I/3I_b = 0.05$, and that the beam damping factor $\delta_E = 0.01$. The solid-line curve of Fig. 17 shows the force transmissibility T_{F12} predicted by Eq. 203; the chain- and dashed-line curves show how T_{F12} changes if either the moment of inertia I of the loading mass or the applied bending moment becomes zero [$\sigma = 0$ or $f(\omega) = 0$, respectively]. Clearly apparent from the two lower curves are the beneficial reductions in T_{F12} that result from the introduction of I.

10.3 Cantilever Beam with an Arbitrarily Located Mass Load

Figure 18 shows a stanchion or vertical cantilever beam that comprises an upper stage of cross-sectional area A_1 and length $\mu\ell$, and a lower stage of cross-sectional area $A_2 = \iota_{12}^{-1} A_1$ and length $(1 - \mu)\ell$. The densities ρ and complex Young's moduli of the two stages are assumed to be identical. If required, the choice of different values for A_1 and A_2 can provide a first approximation to the performance of a tapered stanchion of total height ℓ. Located at the point of juncture of the two stages is a mass load $M = \gamma M_b$, where

$$M_b = \rho A_1 \ell \left[\mu + (1 - \mu)(\iota_{12})^{-1}\right] \tag{207}$$

is the beam mass. The moment of inertia of M is assumed to be negligible. The wavenumbers and the parameters ϵ^* (Eq. 148) of the two stages are conveniently related as follows:

$$n_2^*/n_1^* = (r_{g1}/r_{g2})^{\frac{1}{2}} = \nu_{12} \tag{208}$$

and

$$\frac{\epsilon_2^*}{\epsilon_1^*} = \frac{A_2 r_{g2}^2 (n_2^*)^2}{A_1 r_{g1}^2 (n_1^*)^2} = \frac{1}{\iota_{12}\nu_{12}^2} \quad , \tag{209}$$

where r_{g1} and r_{g2} are the radii of gyration of the beam cross sections of areas A_1 and A_2.

If the free end of the stanchion is driven horizontally by a vibratory force $\tilde{F}_1$, it is possible to write

$$\{\Gamma_1\} = \Pi_1\Pi_2\Pi_3 \{\Gamma_2\} = \Pi \{\Gamma_2\} \quad , \tag{210}$$

where

$$\{\Gamma_1\} = \begin{bmatrix} \tilde{F}_1 \\ \tilde{V}_1 \\ 0 \\ \tilde{\theta}_1 \end{bmatrix} \tag{211}$$

and

$$\{\Gamma_2\} = \begin{bmatrix} \tilde{\Gamma}_2 \\ 0 \\ \tilde{B}_2 \\ 0 \end{bmatrix} . \tag{212}$$

In addition, the matrices Π_1 and Π_3 are given by Eq. 163 in which the relevant arguments are now $\mu n_1^* \ell = N_1^* \ell$ and $(1 - \mu) n_2^* \ell = (1 - \mu)\nu_{12} n_1^* \ell = N_2^* \ell$, respectively; that is,

$$\Pi_1 = \tfrac{1}{2} \begin{bmatrix} T_{11}^* & -n_1^* \epsilon_1^* T_{31}^* & -n_1^* T_{41}^* & \epsilon_1^* T_{21}^* \\ \frac{-1}{n_1^* \epsilon_1^*} T_{41}^* & T_{11}^* & \frac{1}{\epsilon_1^*} T_{21}^* & \frac{-1}{\mu_1^*} T_{31}^* \\ \frac{-1}{n_1^*} T_{31}^* & \epsilon_1^* T_{21}^* & T_{11}^* & \frac{-\epsilon_1^*}{n_1^*} T_{41}^* \\ \frac{1}{\epsilon_1^*} T_{21}^* & -n_1^* T_{41}^* & \frac{-n_1^*}{\epsilon_1^*} T_{31}^* & T_{11}^* \end{bmatrix} \tag{213}$$

and

$$\Pi_3 = \begin{bmatrix} T_{12}^* & \cdot & -n_2^* T_{42}^* & \cdot \\ \frac{-1}{n_2^* \epsilon_2^*} T_{42}^* & \cdot & \frac{1}{\epsilon_2^*} T_{22}^* & \cdot \\ \frac{-1}{n_2^*} T_{32}^* & \cdot & T_{12}^* & \cdot \\ \frac{1}{\epsilon_2^*} T_{22}^* & \cdot & \frac{-n_2^*}{\epsilon_2^*} T_{32}^* & \cdot \end{bmatrix} , \tag{214}$$

where

$$T_{1i}^* = (\text{ch.+c.})_{N_i^* \ell} , \tag{215}$$

$$T_{2i}^* = (\text{ch.-c.})_{N_i^* \ell} , \tag{216}$$

$$T_{3i}^* = (\text{sh.+c.})_{N_i^* \ell} , \tag{217}$$

and

$$T_{4i}^* = (\text{sh.-s.})_{N_i^* \ell} . \qquad (i = 1,2) \tag{218}$$

Consequently, because Π_2 is the transmission matrix of the lumped mass M (Eq. 131), it is possible to state that

$$\Pi_2\Pi_3 = \tfrac{1}{2}\begin{bmatrix} \Delta_{12}^* & \cdot & -n_2^*\Delta_{42}^* & \cdot \\ -\frac{1}{n_2^*\epsilon_2^*}T_{42}^* & \cdot & \frac{1}{\epsilon_2^*}T_{22}^* & \cdot \\ -\frac{1}{n_2^*}T_{32}^* & \cdot & T_{12}^* & \cdot \\ \frac{1}{\epsilon_2^*}T_{22}^* & \cdot & \frac{-n_2^*}{\epsilon_2^*}T_{32}^* & \cdot \end{bmatrix} \tag{219}$$

and

$$\Pi = \Pi_1\Pi_2\Pi_3 = \tfrac{1}{2}\begin{bmatrix} \alpha_{11} & \cdot & \alpha_{13} & \cdot \\ \alpha_{21} & \cdot & \alpha_{23} & \cdot \\ \alpha_{31} & \cdot & \alpha_{33} & \cdot \\ \alpha_{41} & \cdot & \alpha_{43} & \cdot \end{bmatrix} , \tag{220}$$

where

$$\Delta_{12}^* = (T_{12}^* + \mu_m^* T_{42}^*) \quad , \tag{221}$$

$$\Delta_{42}^* = (T_{42}^* + \mu_m^* T_{22}^*) \quad , \tag{222}$$

$$\alpha_{11} = \tfrac{1}{2}\,(T_{11}^*\Delta_{12}^* + \nu_{12}\iota_{12}T_{31}^*T_{42}^* + \nu_{12}^{-1}T_{41}^*T_{32}^* + \nu_{12}^2\iota_{12}T_{21}^*T_{22}^*) \quad , \tag{223}$$

$$\alpha_{21} = -\frac{1}{2n_1^*\epsilon_1^*}\,(T_{41}^*\Delta_{12}^* + \nu_{12}\iota_{12}T_{11}^*T_{42}^* + \nu_{12}^{-1}T_{21}^*T_{32}^* + \nu_{12}^2\iota_{12}T_{31}^*T_{22}^*) \quad , \tag{224}$$

$$\alpha_{31} = -\frac{1}{2n_1^*}\left(T_{31}^*\Delta_{12}^* + \nu_{12}\iota_{12}T_{21}^*T_{42}^* + \nu_{12}^{-1}T_{11}^*T_{32}^* + \nu_{12}^2\iota_{12}T_{41}^*T_{22}^*\right) \quad , \tag{225}$$

$$\alpha_{41} = \frac{1}{2\epsilon_1^*}\left(T_{21}^*\Delta_{12}^* + \nu_{12}\iota_{12}T_{41}^*T_{42}^* + \nu_{12}^{-1}T_{31}^*T_{32}^* + \nu_{12}^2\iota_{12}T_{11}^*T_{22}^*\right) \quad , \tag{226}$$

$$\alpha_{13} = -\frac{n_1^*}{2}\left(T_{41}^*T_{12}^* + \nu_{12}^3\iota_{12}T_{21}^*T_{32}^* + \nu_{12}T_{11}^*\Delta_{42}^* + \nu_{12}^2\iota_{12}T_{31}^*T_{22}^*\right) \quad , \tag{227}$$

$$\alpha_{23} = \frac{1}{2\epsilon_1^*}\left(T_{21}^*T_{12}^* + \nu_{12}^3\iota_{12}T_{31}^*T_{32}^* + \nu_{12}T_{41}^*\Delta_{42}^* + \nu_{12}^2\iota_{12}T_{11}^*T_{22}^*\right) \quad , \tag{228}$$

$$\alpha_{33} = \frac{1}{2}\left(T_{11}^*T_{12}^* + \nu_{12}^3\iota_{12}T_{41}^*T_{32}^* + \nu_{12}T_{31}^*\Delta_{42}^* + \nu_{12}^2\iota_{12}T_{21}^*T_{22}^*\right) \quad , \tag{229}$$

and

$$\alpha_{43} = \frac{-n_1^*}{2\epsilon_1^*}\left(T_{31}^*T_{12}^* + \nu_{12}^3\iota_{12}T_{11}^*T_{32}^* + \nu_{12}T_{21}^*\Delta_{42}^* + \nu_{12}^2\iota_{12}T_{41}^*T_{22}^*\right) \quad ; \tag{230}$$

in Eqs. 221 and 222,

$$\mu_m^* = \frac{j\omega M}{n_2^*\epsilon_2^*} = \gamma(n_1^*\ell)\,\nu_{12}\left[\mu\iota_{12} + (1-\mu)\right] \quad . \tag{231}$$

Because there is no bending moment applied to the beam, Eqs. 175-178 for impedance and transmissibility are applicable here and, in fact, they may be simplified because the beam is rigidly terminated ($Z_T = Z_P = \infty$); for example, Eqs. 175 and 177 for driving-point impedance Z_1 and force transmissibility T_{F12} reduce to Eqs. 182 and 183, which are phrased concisely in terms of

the foregoing parameters α. The Eqs. 223-230 for these parameters also simplify for a uniform stanchion having stages of identical cross-sectional areas and identical radii of gyration, because then $n_2^* = n_1^* = n^*$, $\epsilon_2^* = \epsilon_1^* = \epsilon^*$, and $\nu_{12} = \iota_{12} = 1.0$. Should the beam be loaded in this case by a dynamic absorber of impedance Z_a (Eq. 123), rather than by a lumped mass $M = \gamma M_b$, then the expression for μ_m^*, which reduces to

$$\mu_m^* = \gamma(n^* \ell) \quad , \tag{232}$$

can be replaced by

$$\mu_m^* = \frac{Z_a}{j\omega M_b}(n^* \ell) \quad ; \tag{233}$$

no other modification is necessary.

Representative calculations of the force transmissibility across a uniform stanchion have been made from Eq. 183 in which the foregoing parameters α were substituted after simplification. The stanchion is loaded by a mass $M = 10\ M_b (\gamma = 10)$ that is consecutively positioned where $\mu = 0$, 0.1, and 0.9 (Fig. 18). The resultant transmissibility curves are plotted in Fig. 19 on a scale that is proportional to $\sqrt{\omega}$; the dashed-line curve shows the transmissibility in the absence of M. In all cases, the beam damping factor $\delta_E = 0.01$.

When $\mu = 0$, transmissibility T_{F12} falls off rapidly as frequency increases, in the manner that has come to be associated with mass-loaded structures, the effectiveness of added mass in reducing transmissibility being fully apparent. However, the unexpected result is noted that when $\mu = 0.1$ (chain-line curve), the reduction in T_{F12} is much less than when

$\mu = 0$. Whereas at low frequencies T_{F12} remains < 1.0 following the initial beam resonance, at higher frequencies T_{F12} closely approaches the level of T_{F12} noted when $\gamma = 0$ (dashed-line curve). Moreover, when $\mu = 0.9$ (upper solid-line curve for which M lies near the botton of the stanchion), force is amplified ($T_{F12} > 1.0$) at all frequencies, and the use of additional mass must be considered detrimental. Clearly implied here is the importance of introducing mass for vibration control only when it can be located directly in opposition to the impressed force.

Another possible disadvantage to mass loading the stanchion or other cantilever beam near its root is demonstrated by the curves of Fig. 20, where frequency ratios ω_2/ω_1 and ω_3/ω_1 are plotted versus μ, the parameter that controls the distance of the loading mass from the free end of the beam. Here, ω_1, ω_2, and ω_3 are the first three resonant frequencies of a uniform beam, which is loaded, for example, by a mass $M = 0.25\ M_b$. Both ω_2 and ω_3 become harmonics of ω_1 when μ is slightly greater than 0.8, a fact that can be detrimental to effective vibration control, although it has proven fortuitous in musical applications.[38] The frequency ω_2, for example, also becomes a harmonic of ω_1 when $\mu \approx 0.30$ and 0.41.

10.4 Mass-Loaded Three-Stage Cantilever Beam

Consider, finally, a cantilever beam that is mass loaded and driven by a vibratory force at its free end; the beam comprises three stages of arbitrary lengths and arbitrary but uniform cross-sectional areas A_1, A_2, and A_3, as in Fig. 21. A similar three-stage beam without a mass load has been considered in Refs. 39 and 40. It is assumed here that the densities ρ and complex Young's moduli E^* of each beam stage are

identical--and that there exists continuity of force and bending moment, and continuity of translational and rotational velocity, where the beam stages are connected at distances of $\mu_1 \ell$ and $\mu_2 \ell$ from the driving point. The far end of the beam is rigidly terminated so that Eqs. 182 and 183 for driving-point impedance Z_1 and force transmissibility T_{F12} remain applicable.

The wavenumbers of the beam stages, and the parameters

$$\epsilon_i^* = -E^* A_i r_{gi}^2 (n_i^*)^2/j\omega \qquad (i = 1,2,3) \qquad (234)$$

are conveniently related as in Sec. 10.3; thus,

$$n_2^*/n_1^* = (r_{g1}/r_{g2})^{\frac{1}{2}} = \nu_{12} \quad , \qquad (235)$$

$$n_3^*/n_1^* = (r_{g1}/r_{g3})^{\frac{1}{2}} = \nu_{13} \quad , \qquad (236)$$

and

$$\frac{\epsilon_2^*}{\epsilon_1^*} = \frac{A_2 r_{g2}^2 (n_2^*)^2}{A_1 r_{g1}^2 (n_1^*)^2} = \frac{1}{\iota_{12}\nu_{12}^2} \quad , \qquad (237)$$

$$\frac{\epsilon_3^*}{\epsilon_2^*} = \frac{A_3 r_{g3}^2 (n_3^*)^2}{A_2 r_{g2}^2 (n_2^*)^2} = \frac{\iota_{12}\nu_{12}^2}{\iota_{13}\nu_{13}^2} \quad , \qquad (238)$$

where

$$\iota_{12} = A_1/A_2 \quad , \qquad (239)$$

$$\iota_{13} = A_1/A_3 \quad , \qquad (240)$$

and r_{gi} are the radii of gyration of the beam cross sections of areas A_i $(i = 1,2,3)$. As before, it is convenient to define a mass ratio $\gamma = M/M_b$, where the beam mass

$$M_b = \rho A_1 \ell \left[\mu_1 + (\mu_2 - \mu_1)(\iota_{12})^{-1} + (1 - \mu_2)(\iota_{13})^{-1}\right] = \rho A_1 \ell U \quad . \tag{241}$$

It can now be stated that

$$\{\Gamma_1\} = \Pi_0 \Pi_1 \Pi_2 \Pi_3 \{\Gamma_2\} = \Pi \{\Gamma_2\} \quad , \tag{242}$$

where $\{\Gamma_1\}$ and $\{\Gamma_2\}$ are given by Eqs. 211 and 212; Π_1 is given by Eq. 213; Π_2 is also given by Eq. 213 in which the second subscript to the parameters T^* is always 2 rather than 1, and in which $n_1^* \rightarrow n_2^*$, $\epsilon_1^* \rightarrow \epsilon_2^*$;

$$\Pi_3 = \tfrac{1}{2}\begin{bmatrix} T_{13}^* & \cdot & -n_3^* T_{43}^* & \cdot \\ \dfrac{-1}{n_3^* \epsilon_3^*} T_{43}^* & \cdot & \dfrac{1}{\epsilon_3^*} T_{23}^* & \cdot \\ \dfrac{-1}{n_3^*} T_{33}^* & \cdot & T_{13}^* & \cdot \\ \dfrac{1}{\epsilon_3^*} T_{23}^* & \cdot & \dfrac{-n_3^*}{\epsilon_3^*} T_{33}^* & \cdot \end{bmatrix} \quad ; \tag{243}$$

and

$$\Pi = \tfrac{1}{2}\begin{bmatrix} \alpha_{11} & \cdot & \alpha_{13} & \cdot \\ \alpha_{21} & \cdot & \alpha_{23} & \cdot \\ \alpha_{31} & \cdot & \alpha_{33} & \cdot \\ \alpha_{41} & \cdot & \alpha_{43} & \cdot \end{bmatrix} \quad . \tag{244}$$

The parameters T^* of the transmission matrices Π_1, Π_2, and Π_3, are defined by Eqs. 215-218 in which i = 1, 2, 3, $N_1^*\ell = \mu n_1^*\ell$, $N_2^*\ell = (\mu_2 - \mu_1)n_2^*\ell = \nu_{12}(\mu_2 - \mu_1)n_1^*\ell$, and $N_3^*\ell = (1 - \mu_2)n_3^*\ell = \nu_{13}(1 - \mu_2)n_1^*\ell$. When the product of the matrices $\Pi_1\Pi_2\Pi_3$ is multiplied by the square transmission matrix Π_0 of the loading mass M (Eq. 131), the following expressions for the complex parameters α are obtained:

$$\alpha_{11} = \frac{1}{4}\left(\Psi_{11}^* + \mu_m^*\alpha_{21}\right) \quad , \tag{245}$$

$$\alpha_{21} = \frac{-1}{4n_1^*\epsilon_1^*}\left(T_{41}^*\Lambda_{11}^* + \nu_{12}\iota_{12}T_{11}^*\Lambda_{21}^* + \nu_{12}^{-1}T_{21}^*\Lambda_{31}^* + \nu_{12}^2\iota_{12}T_{31}^*\Lambda_{41}^*\right) \quad , \tag{246}$$

$$\alpha_{31} = \frac{-1}{4n_1^*}\left(T_{31}^*\Lambda_{11}^* + \nu_{12}\iota_{12}T_{21}^*\Lambda_{21}^* + \nu_{12}^{-1}T_{11}^*\Lambda_{31}^* + \nu_{12}^2\iota_{12}T_{41}^*\Lambda_{41}^*\right) \quad , \tag{247}$$

$$\alpha_{41} = \frac{1}{4\epsilon_1^*}\left(T_{21}^*\Lambda_{11}^* + \nu_{12}\iota_{12}T_{41}^*\Lambda_{21}^* + \nu_{12}^{-1}T_{31}^*\Lambda_{31}^* + \nu_{12}^2\iota_{12}T_{11}^*\Lambda_{41}^*\right) \quad , \tag{248}$$

$$\alpha_{13} = \frac{-n_1^*}{4}\left(\Psi_{13}^* + \mu_m^*\alpha_{23}\right) \quad , \tag{249}$$

$$\alpha_{23} = \frac{1}{4\epsilon_1^*}\left(T_{21}^*\Lambda_{33}^* + \nu_{12}T_{41}^*\Lambda_{13}^* + \nu_{12}^2\iota_{12}T_{11}^*\Lambda_{23}^* + \nu_{12}^3\iota_{12}T_{31}^*\Lambda_{43}^*\right) \quad , \tag{250}$$

$$\alpha_{33} = \frac{1}{4}\left(T_{11}^*\Lambda_{33}^* + \nu_{12}T_{31}^*\Lambda_{13}^* + \nu_{12}^2\iota_{12}T_{21}^*\Lambda_{23}^* + \nu_{12}^3\iota_{12}T_{41}^*\Lambda_{43}^*\right) \quad , \tag{251}$$

and

$$\alpha_{43} = \frac{-n_1^*}{4\epsilon_1^*}\left(T_{31}^*\Lambda_{33}^* + \nu_{12}T_{21}^*\Lambda_{13}^* + \nu_{12}^2\iota_{12}T_{41}^*\Lambda_{23}^* + \nu_{12}^3\iota_{12}T_{11}^*\Lambda_{43}^*\right) \quad , \tag{252}$$

where

$$\Psi_{11}^* = \left(T_{11}^*\Lambda_{11}^* + \nu_{12}\iota_{12}T_{31}^*\Lambda_{21}^* + \nu_{12}^{-1}T_{41}^*\Lambda_{31}^* + \nu_{12}^2\iota_{12}T_{21}^*\Lambda_{41}^*\right) \quad , \tag{253}$$

$$\Psi_{13}^* = \left(T_{41}^*\Lambda_{33}^* + \nu_{12}T_{11}^*\Lambda_{13}^* + \nu_{12}^2\iota_{12}T_{31}^*\Lambda_{23}^* + \nu_{12}^3\iota_{12}T_{21}^*\Lambda_{43}^*\right) \quad , \tag{254}$$

and

$$\mu_m^* = \gamma(n_1^*\ell)U \quad . \tag{255}$$

In the foregoing equations,

$$\Lambda_{11}^* = \left(T_{12}^*T_{13}^* + u\,T_{32}^*T_{43}^* + v^{-1}T_{42}^*T_{33}^* + uv\,T_{22}^*T_{23}^*\right) \quad , \tag{256}$$

$$\Lambda_{21}^* = \left(T_{42}^*T_{13}^* + u\,T_{12}^*T_{43}^* + v^{-1}T_{22}^*T_{33}^* + uv\,T_{32}^*T_{23}^*\right) \quad , \tag{257}$$

$$\Lambda_{31}^* = \left(T_{32}^*T_{13}^* + u\,T_{22}^*T_{43}^* + v^{-1}T_{12}^*T_{33}^* + uv\,T_{42}^*T_{23}^*\right) \quad , \tag{258}$$

$$\Lambda_{41}^* = \left(T_{22}^*T_{13}^* + u\,T_{42}^*T_{43}^* + v^{-1}T_{32}^*T_{33}^* + uv\,T_{12}^*T_{23}^*\right) \quad , \tag{259}$$

$$\Lambda_{13}^* = \left(T_{42}^*T_{13}^* + v\,T_{12}^*T_{43}^* + uv\,T_{32}^*T_{23}^* + uv^2\,T_{22}^*T_{33}^*\right) \quad , \tag{260}$$

$$\Lambda_{23}^* = \left(T_{22}^*T_{13}^* + v\,T_{42}^*T_{43}^* + uv\,T_{12}^*T_{23}^* + uv^2\,T_{32}^*T_{33}^*\right) \quad , \tag{261}$$

$$\Lambda_{33}^* = \left(T_{12}^*T_{13}^* + v\,T_{32}^*T_{43}^* + uv\,T_{22}^*T_{23}^* + uv^2\,T_{42}^*T_{33}^*\right) \quad , \tag{262}$$

and

$$A_{43}^{*} = (T_{32}^{*}T_{13}^{*} + v\,T_{22}^{*}T_{43}^{*} + uv\,T_{42}^{*}T_{23}^{*} + uv^{2}\,T_{12}^{*}T_{33}^{*}) \quad , \tag{263}$$

where

$$u = (\iota_{13}\nu_{13}/\iota_{12}\nu_{12}) \tag{264}$$

and

$$v = \nu_{12}^{-1}\nu_{13} \quad . \tag{265}$$

From knowledge of the complex parameters α (Eqs. 245-252), the driving-point impedance Z_1 and transmissibility T_{F12} of a mass-loaded three-stage beam can be calculated from Eqs. 182 and 183 in terms of the wavenumber n_1^* of the first stage. However, to compare the effects of changing the cross-sectional geometry of the beam, and the relative length of its stages, it is helpful to calculate impedance and transmissibility in terms of the wavenumber n_u^* of a uniform reference beam having the same length ℓ, density ρ, and mass M_b as the beam under consideration. The cross-sectional area of this uniform beam is readily shown to be

$$A_u = A_1 U \quad , \tag{266}$$

where U is given by Eq. 241.

Attention is first directed here to three-stage beams having rectangular and uniform outer cross-sectional dimensions. The intermediate stages of the beams are slotted centrally in either the vertical or horizontal direction. In the first case [Fig. 12(a)], every beam stage has the common depth $d_1 = A_u/w_1 U$, where w_1 is the outer width of the beam, and

$$\nu_{12} = \nu_{13} = \iota_{13} = 1.0 \quad . \tag{267}$$

If the corresponding uniform reference beam also has rectangular cross section and depth $d_u = d_1$, it can simply be stated that

$$n_u^* \ell = n_1^* \ell \sqrt{(d_1/d_u)} = n_1^* \ell \quad . \tag{268}$$

In the second case [Fig. 22(b)], every beam stage shares the width $w_1 = A_u/d_1 U$, and

$$\nu_{13} = \iota_{13} = 1.0 \quad ; \tag{269}$$

it can also be demonstrated that

$$\nu_{12} = \sqrt{[d_1/(d_2^2 - 3d_2 d_1 + 3d_1^2)^{\frac{1}{2}}]} \quad , \tag{270}$$

where the solid portions of the intermediate stage have the total depth d_2. In addition, if the corresponding uniform beam has rectangular cross section and width w_1, reference to Eq. 266 shows that

$$n_u^* \ell = n_1^* \ell \sqrt{(d_1/d_u)} = n_1^* \ell / \sqrt{U} \quad . \tag{271}$$

If the beam is "bridle jointed," as in Fig. 22(c), Eq. 270 simply becomes

$$\nu_{12} = \sqrt{(d_1/d_2)} \quad . \tag{272}$$

The force transmissibility T_{F12} across an unloaded beam for which $\mu_1 = 0.5$ and $\mu_2 = 0.9$ is plotted as the upper solid-line curve in Fig. 23. The intermediate beam stage is slotted horizontally, as in Fig. 22(b), and the depth $d_2 = d_1/4$; consequently, the parameters $\nu_{12} = 2/(37)^{\frac{1}{2}} = 0.8109$, and $\iota_{12} = 4$. The transmissibility T_{F12} across the same beam loaded by 5 times its own mass ($\gamma = M/M_b = 5$) is plotted as the lower solid-line curve. For comparison, the transmissibility T_{F12} across an unloaded uniform beam is shown by the dashed-line curve, and T_{F12} across the bridle-jointed beam of Fig. 22(c)--for which μ_1, μ_2, and d_2 take their foregoing values, and $\nu_{12} = 2$ and $\gamma = 0$--is shown by the chain-line curve. In all cases, T_{F12} is plotted versus the dimensionless parameter $n_u^* \ell$, which is proportional to $\sqrt{\omega}$. The beam damping factors $\delta_E = 0.01$.

Of interest are the regions of attenuation ($T_{F12} < 1.0$) that occur in the chain-line curve at frequencies intermediate to the beam resonances. Thus, a maximum attenuation of 4.7 dB is noted between the first and second beam resonances within bounds that differ by a factor of 4.5 in frequency; and maximum attenuations of 15.0 and 12.8 dB are noted between the second and third, and the third and fourth, resonances within bounds that differ by factors of 4.1 and 1.9 in frequency, respectively.

ACKNOWLEDGMENTS

The assistance of Adah A. Wolfe in obtaining the results of Figs. 12, 17, 19, 20, and 23, and the data of Tables I and II, is acknowledged with gratitude. The investigation was sponsored jointly by the U. S. Naval Sea Systems Command and the U. S. Office of Naval Research.

REFERENCES

1. E. A. Guillemin, Communication Networks, Vol. II (Wiley, New York, 1947).

2. L. C. Peterson, "Equivalent Circuits of Linear Active Four-Terminal Networks" Bell System Tech. J. 27, 593-622 (1948).

3. M. B. Reed, Electrical Network Synthesis (Prentice-Hall, Englewood Cliffs, New Jersey, 1955).

4. E. Weber, Linear Transient Analysis, Vol. II (Wiley, New York, 1956).

5. L. A. Pipes, Applied Mathematics for Engineers and Physicists (McGraw-Hill, New York, 1958).

6. M. E. Van Valkenburg, Introduction to Modern Network Synthesis (Wiley, New York, 1960).

7. C. T. Malloy, "Application of Four-Pole Parameters to Torsional Vibration Problems," J. Engr. Ind., Trans. ASME 84, Ser. B, 21-34 (1962).

8. T. E. Kriewall, "A Network Approach to Vibration Analysis," (The University of Michigan College of Engineering Rept. to the Office of Naval Research, No. N6onr-23219, 1957).

9. C. T. Malloy, "Use of Four-Pole Parameters in Vibration Calculations," J. Acoust. Soc. Am. 29, 842-853 (1957).

10. C. T. Malloy, "Four-Pole Parameters in Vibration Analysis," contribution to Mechanical Impedance Methods for Mechanical Vibrations, R. Plunkett, ed. (American Society of Mechanical Engineers, New York, 1958), Sec. 4.

REFERENCES (CONTINUED)

11. J. E. Ruzicka and R. D. Cavanaugh, "Vibration Isolation of Nonrigid Bodies," contribution to Mechanical Impedance Methods for Mechanical Vibrations, R. Plunkett, ed. (American Society of Mechanical Engineers, New York, 1958), Sec. 9.

12. E. L. Hixson, "Mechanical Impedance and Mobility," contribution to Shock and Vibration Handbook, C. M. Harris and C. E. Crede, eds. (McGraw-Hill, New York, 1961), Chap. 10.

13. W. C. L. Hu and D. D. Kana, "Four-Pole Parameters for Impedance Analyses of Conical and Cylindrical Shells Under Axial Excitations," J. Acoust. Soc. Am. 43, 683-690 (1968).

14. J. C. Snowdon, "Mechanical Four-Pole Parameters and their Application," J. Sound Vib. 15, 307-323 (1971).

15. K. Marguerre, "Matrices of Transmission in Beam Problems," contribution to Progress in Solid Mechanics, Vol. I, I. N. Sneddon and R. Hill, eds. (Interscience, New York, 1960), Chap. 2.

16. D. F. Miller, "Forced, Steady-State Vibration Analysis of a Cantilever Beam with an Impedance Type Wall by Use of a Transfer Matrix," Westinghouse Res. Lab. Rept. 107-3000-R1 (March 1961).

17. E. C. Pestel and F. A. Leckie, Matrix Methods in Elastomechanics (McGraw-Hill, New York, 1963).

18. S. Rubin, "Transmission Matrices for Vibration and Their Relation to Admittance and Impedance," J. Eng. Ind., Trans. ASME 86, Ser. B, 9-21 (1964).

19. M. Konno and H. Nakamura, "Equivalent Electrical Network for the Transversely Vibrating Bar," J. Acoust. Soc. Am. 38, 614-622 (1965).

REFERENCES (CONTINUED)

20. H. Lee, "Optimum Modelling of Structures to Predict Dynamic Elastic Response," thesis submitted to The Pennsylvania State University in partial fulfillment of the requirements for the Ph.D. Degree in Engineering Mechanics, June 1966.

21. R. D. Henshell and G. B. Warburton, "Transmission of Vibration in Beam Systems," Int. J. Num. Methds. Eng. 1, 47-66 (1969).

22. Y. K. Lin and B. K. Donaldson, "A Brief Survey of Transfer Matrix Techniques with Special Reference to the Analysis of Aircraft Panels," J. Sound Vib. 10, 103-143 (1969).

23. A. O. Sykes, "Application of Admittance and Impedance Concepts in the Synthesis of Vibrating Systems," contribution to Synthesis of Vibrating Systems, edited by V. H. Neubert and J. P. Raney (American Society of Mechanical Engineers, New York, November, 1971) Chapter 3, pp. 22-37.

24. M. Harrison, A. O. Sykes, and M. Martin, "Wave Effects in Isolation Mounts," J. Acoust. Soc. Am. 24, 62-71 (1952).

25. S. H. Crandall, "Mechanical Vibrations with Deterministic Excitation," contribution to Random Vibrations, S. H. Crandall, ed. (Wiley, New York, 1959), Chap. 1.

26. C. E. Crede, Shock and Vibration Concepts in Engineering Design (Prentice-Hall, Englewood Cliffs, New Jersey, 1965).

27. J. C. Snowdon, Vibration and Shock in Damped Mechanical Systems (Wiley, New York, 1968).

28. J. C. Snowdon, "Forced Vibration of Internally Damped Circular Plates with Supported and Free Boundaries," J. Acoust. Soc. Am. 47, 882-891 (1970).

REFERENCES (CONTINUED)

29. I. I. Klyukin, "Attenuation of Flexural Waves in Rods and Plates by Means of Resonance Vibrating Systems," Soviet Phys. Acoust. 6, 209-215 (1960).

30. H. R. Spence and J. H. Winters, "Application of the Vibration Absorber Principle for the Protection of Airborne Electronic Equipment," Shock. Vib. Bull. 28, Pt. 4, 57-64 (1960).

31. I. I. Klyukin and Y. D. Sergeev, "Scattering of Flexural Waves by Antivibrators on a Plate," Soviet Phys. Acoust. 10, 49-53 (1964).

32. A. D. Nashif, "Development of Practical Tuned Dampers to Operate Over a Wide-Temperature Range," Shock Vib. Bull. 38, Pt. 3, 57-69 (1968).

33. J. Van de Vegte and Y. L. Wu, "Optimal Linear Dampers for Flexible Plates," J. Engr. Ind., Trans. ASME 97, Ser. B, 887-892 (1975).

34. R. H. Scanlan, "A Note on Transverse Bending of Beams Having Both Translating and Rotating Mass Elements," J. Aero. Sci. 15, 425, 426, and 434 (1948).

35. S. Durvasula, "Vibrations of a Uniform Cantilever Beam Carrying a Concentrated Mass and Moment of Inertia at the Tip," J. Aeron. Soc. India 18, 17-25 (1966).

36. T. W. Lee, "Vibration Frequencies for a Uniform Beam with One End Spring-Hinged and Carrying a Mass at the Other Free End," J. Appl. Mech. 40, 813-815 (1973).

37. G. V. Rao and K. K. Raju, "A Galerkin Finite Element Analysis of a Uniform Beam Carrying a Concentrated Mass and Rotary Inertia with a Spring Hinge," J. Sound Vib. 37, 567-569 (1974).

REFERENCES (CONTINUED)

38. B. F. Miessner, "Electronic Piano," U. S. Patent 3,038,362 (June 12, 1962).

39. H. Nakamura and M. Konno, "Resonant Frequency of a Stepped Cantilever," J. Acoust. Soc. Japan 21, 55-64 (1965).

40. R. L. Kerlin, "Transverse Vibration of Uniform and Nonuniform, Internally Damped Cantilever Beams," thesis submitted to The Pennsylvania State University in partial fulfillment of the requirements for the Ph.D. degree in Engineering Acoustics, March, 1972.

Table I. Optimum values of the frequency ratio $(\omega_a/\omega_m)_o$ and the damping ratio $(\delta_R)_o$, and the corresponding values of transmissibility $(T_{Fa})_{max}$, for a dynamic absorber tuned to the fundamental resonance of a circular plate with a clamped boundary.

M_a/M_p	$(\omega_a/\omega_m)_o$	$(\delta_R)_o$	$(T_{Fa})_{max}$
0.025	0.908	0.222	6.304
0.05	0.828	0.306	4.496
0.10	0.698	0.408	3.202
0.25	0.465	0.549	2.086

Table II. Optimum values of the frequency ratio $(\omega_a/\omega_m)_o$ and the damping ratio $(\delta_R)_o$, and the corresponding values of transmissibility $(T_{Fa})_{max}$, for a dynamic absorber tuned to the fundamental resonance of a circular plate with a simply supported boundary.

M_a/M_P	$(\omega_a/\omega_m)_o$	$(\delta_R)_o$	$(T_{Fa})_{max}$
0.025	0.935	0.177	7.227
0.05	0.877	0.244	5.174
0.10	0.779	0.329	3.701
0.25	0.579	0.456	2.407

FIGURE LEGENDS

Fig. 1 General four-terminal system.

Fig. 2 (a) Lumped mass obeying Newton's second law, and (b) a massless spring obeying Hooke's law.

Fig. 3 Series connection of four-terminal systems.

Fig. 4 Parallel connection of four-terminal systems.

Fig. 5 Dashpot obeying Newton's law of viscosity.

Fig. 6 Parallel spring and dashpot.

Fig. 7 Dynamic absorber.

Fig. 8 Mechanical system with a dynamic absorber.

Fig. 9 Uniform thin rod in longitudinal vibration.

Fig. 10 Center-driven Bernoulli-Euler beam in symmetrical transverse vibration.

Fig. 11 Center-driven thin circular plate in transverse vibration.

Fig. 12 Force transmissibility T_{Fa} across the plate of Fig. 11 when it is clamped around its boundary and a dynamic absorber is attached to its midpoint. Mass ratio $\gamma_a = M_a/M_p = 0.1$ and 0.25; for the dashed-line curve, $M_a/M_p = 0$. Plate damping factors $\delta_E = \delta_G = 0.01$.

Fig. 13 (a) Lumped mass, and (b) lumped mass having a finite moment of inertia.

Fig. 14 (a) Spring in cascade, (b) a supported spring, and (c) a dashpot.

Fig. 15 Bernoulli-Euler beam in transverse vibration.

FIGURE LEGENDS (CONTINUED)

Fig. 16 (a) Simply supported beam, (b) spring-supported cantilever beam, and (c) cantilever beam loaded by a mass having a finite moment of inertia. Beam (a) is driven centrally by a sinusoidally varying bending moment; beam (b) is driven at its free end by a sinusoidally varying force; and beam (c) is driven simultaneously at its free end by a sinusoidally varying force and bending moment.

Fig. 17 Force transmissibility T_{F12} across the cantilever beam of Fig. 16(c) when $\gamma = M/M_b = 5$, $\sigma = I/3L_b = 0.05$, and $f(\omega) = 0.5$ (solid-line curve). If the moment of inertia of the loading mass is zero, or if the applied bending moment is zero, T_{F12} is increased or reduced as shown by the chain-line or the dashed-line curve, respectively. Beam damping factor $\delta_E = 0.01$.

Fig. 18 Vertical stanchion or beam that is mass loaded at an arbitrary distance $\mu\ell$ from its free end, where it is driven by a sinusoidally varying force. The beam comprises two stages of different cross-sectional areas.

Fig. 19 Force transmissibility T_{F12} across the beam of Fig. 18 when its component stages have the same cross-sectional area, the mass ratio $\gamma = 10$, and $\mu = 0$, 0.1, and 0.9. The transmissibility across the unloaded beam ($\gamma = 0$) is shown by the dashed-line curve. Beam damping factor $\delta_E = 0.01$.

Fig. 20 Frequency ratios ω_2/ω_1 and ω_3/ω_1 in which ω_1, ω_2, and ω_3 are the first three resonant frequencies of the mass-loaded beam of Fig. 18. The component stages of the beam have the same cross-sectional area; the mass ratio $\gamma = 0.25$.

FIGURE LEGENDS (CONTINUED)

Fig. 21 Mass-loaded cantilever beam driven at its free end by a sinusoidally varying force; the beam comprises three uniform stages of arbitrary cross-sectional areas and arbitrary lengths.

Fig. 22 Mass-loaded three-stage cantilever beams driven at their free ends by a sinusoidally varying force: (a) vertically slotted beam, (b) horizontally slotted beam, and (c) "bridle-connected" beam.

Fig. 23 Force transmissibility T_{F12} across the beam of Fig. 22(b) shown by the upper and lower solid-line curves for which the mass ratio $\gamma = 0$ and 5, respectively; the parameters $\mu_1 = 0.5$, $\mu_2 = 0.9$, and $d_2 = d_1/4$. The force transmissibility across a uniform beam, and across the beam of Fig. 22(c), is shown by the dashed- and chain-line curves for which $\gamma = 0$.

FIG. 1

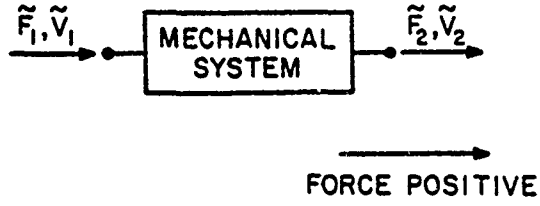

FIG. 2

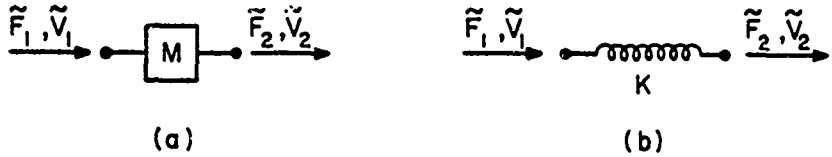

FIG. 3

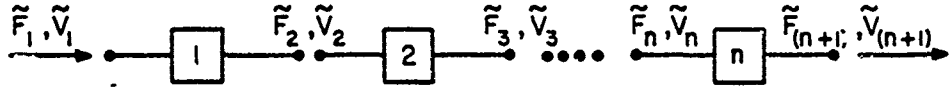

FIG. 4

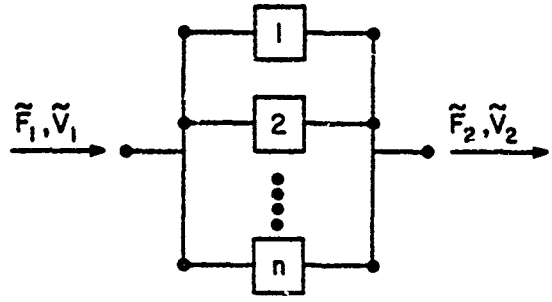
1
2
n
$\tilde{F}_1, \tilde{V}_1$
$\tilde{F}_2, \tilde{V}_2$

FIG. 5

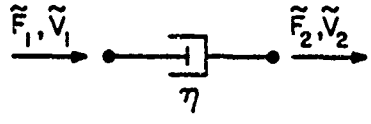
$\tilde{F}_1, \tilde{V}_1$
$\tilde{F}_2, \tilde{V}_2$
η

FIG.6

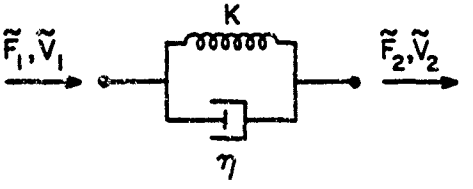
K
$\tilde{F}_1, \tilde{V}_1$
$\tilde{F}_2, \tilde{V}_2$
η

FIG.7

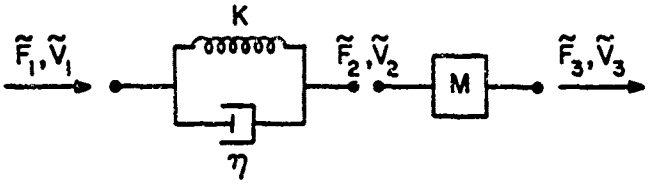
K
$\tilde{F}_1, \tilde{V}_1$
$\tilde{F}_2, \tilde{V}_2$
M
$\tilde{F}_3, \tilde{V}_3$
η

FIG.8

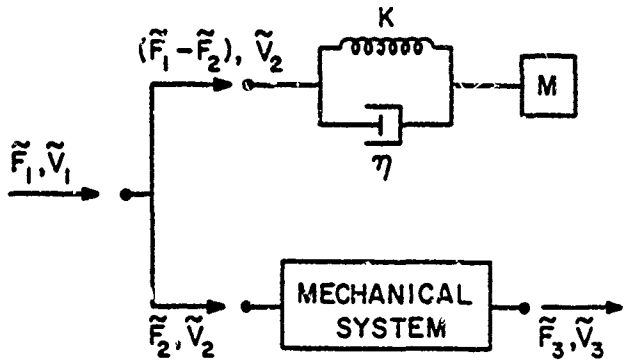
K
$(\tilde{F}_1-\tilde{F}_2)$, $\tilde{V}_2$
M
η
$\tilde{F}_1, \tilde{V}_1$
MECHANICAL SYSTEM
$\tilde{F}_2, \tilde{V}_2$
$\tilde{F}_3, \tilde{V}_3$

FIG.9

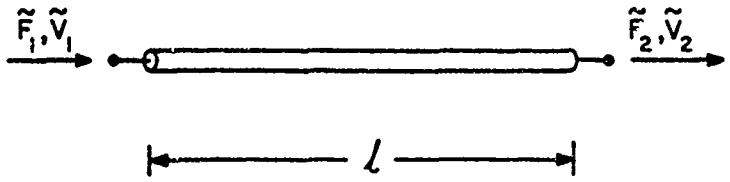
$\tilde{F}_1, \tilde{V}_1$
$\tilde{F}_2, \tilde{V}_2$
l

FIG. 10

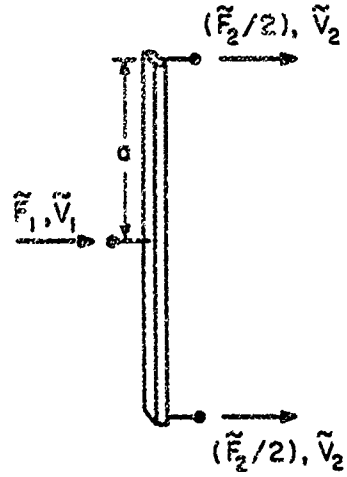
$(\tilde{F}_2/2), \tilde{V}_2$
a
$\tilde{F}_1, \tilde{V}_1$
$(\tilde{F}_2/2), \tilde{V}_2$

FIG. 11

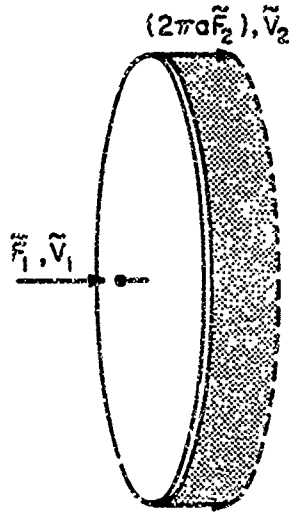
$(2\pi a\tilde{F}_2), \tilde{V}_2$
$\tilde{F}_1, \tilde{V}_1$

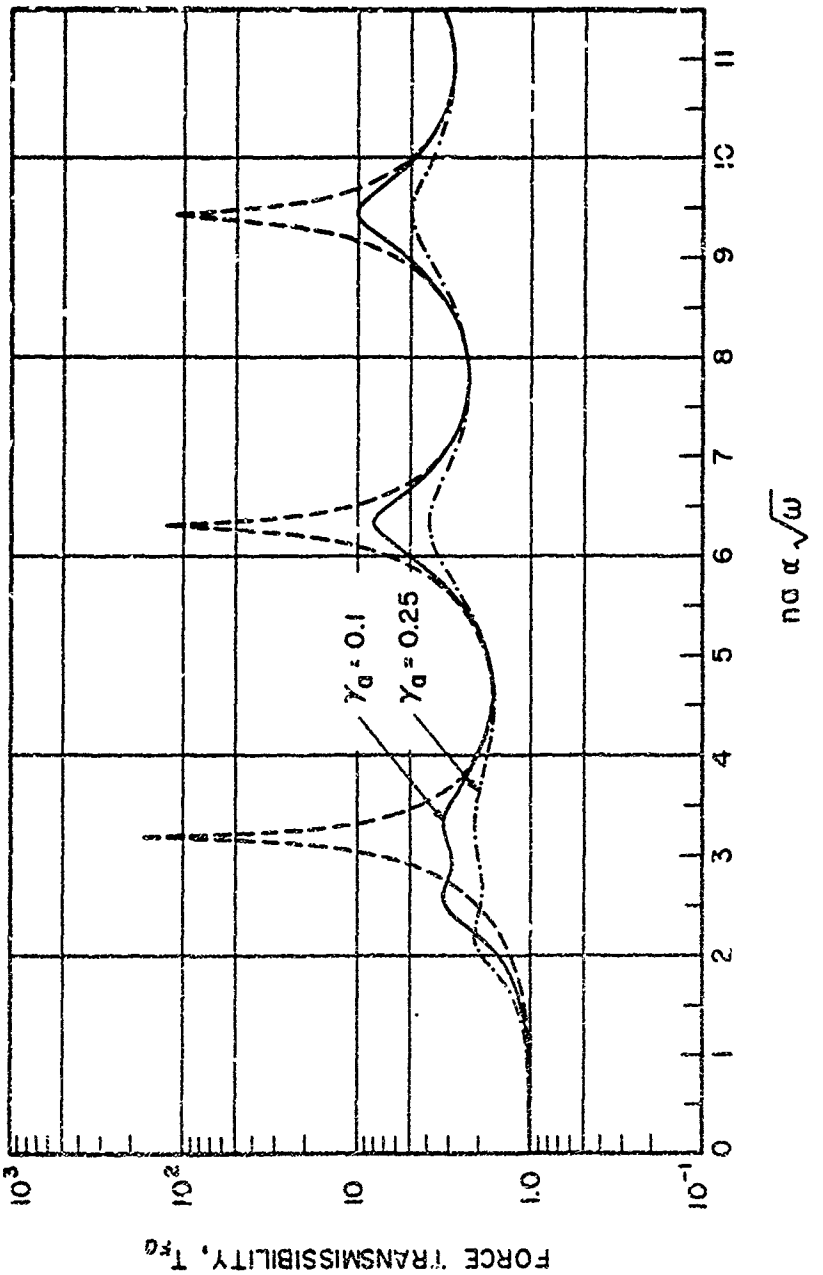
FORCE TRANSMISSIBILITY, T_{FQ}
10^3
10^2
10
1.0
10^{-1}
0
1
2
3
4
5
6
7
8
9
10
11
$\Omega a \propto \sqrt{\omega}$
$\gamma_a = 0.1$
$\gamma_a = 0.25$

FIG.12

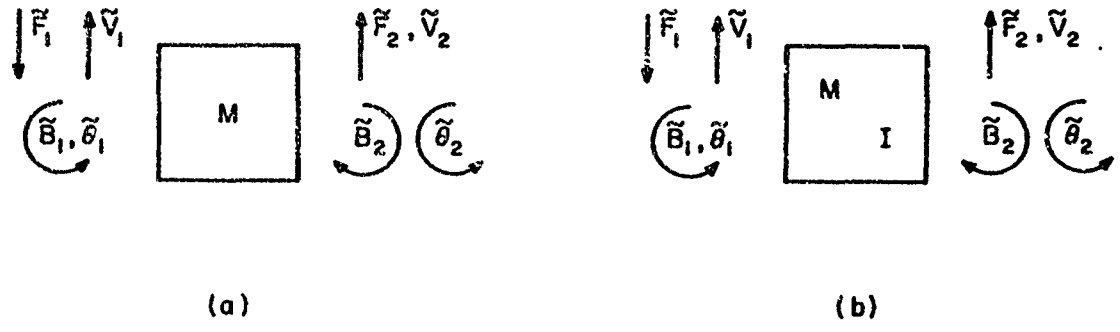
$\tilde{F}_1$
$\tilde{V}_1$
$\tilde{B}_1, \tilde{\theta}_1$
M
$\tilde{F}_2, \tilde{V}_2$
$\tilde{B}_2$
$\tilde{\theta}_2$
(a)
$\tilde{F}_1$
$\tilde{V}_1$
$\tilde{B}_1, \tilde{\theta}_1$
M
I
$\tilde{F}_2, \tilde{V}_2$
$\tilde{B}_2$
$\tilde{\theta}_2$
(b)

FIG.13

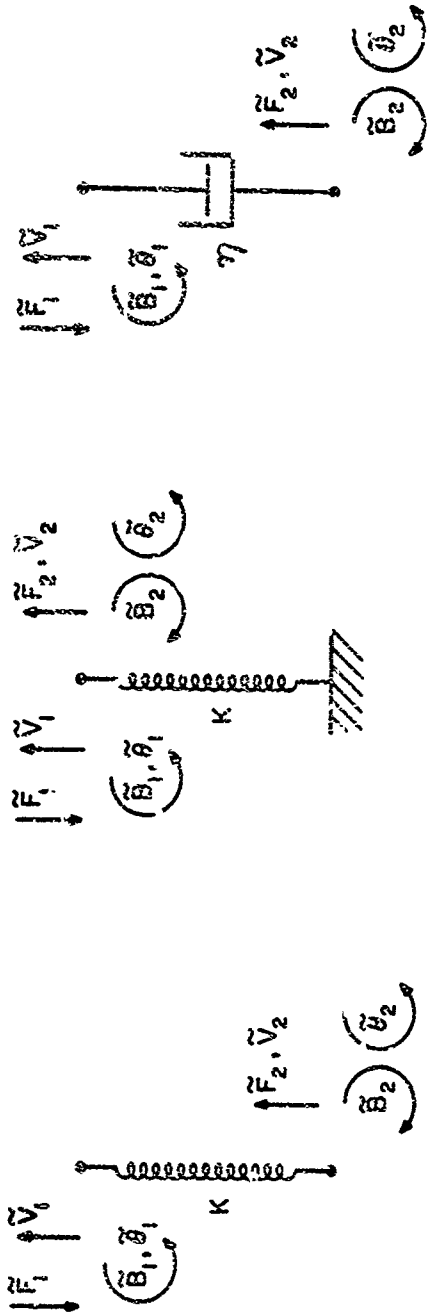

FIG. 14

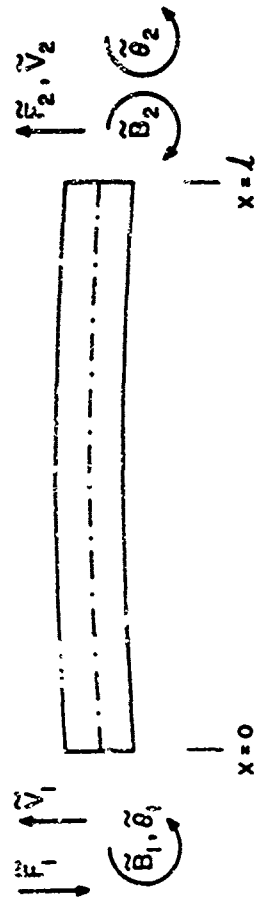
$\tilde{F}_2, \tilde{V}_2$
$\tilde{\theta}_2$
$\tilde{B}_2$
$x = L$
$x = 0$
$\tilde{V}_1$
$\tilde{B}_1, \tilde{\theta}_1$

FIG.15

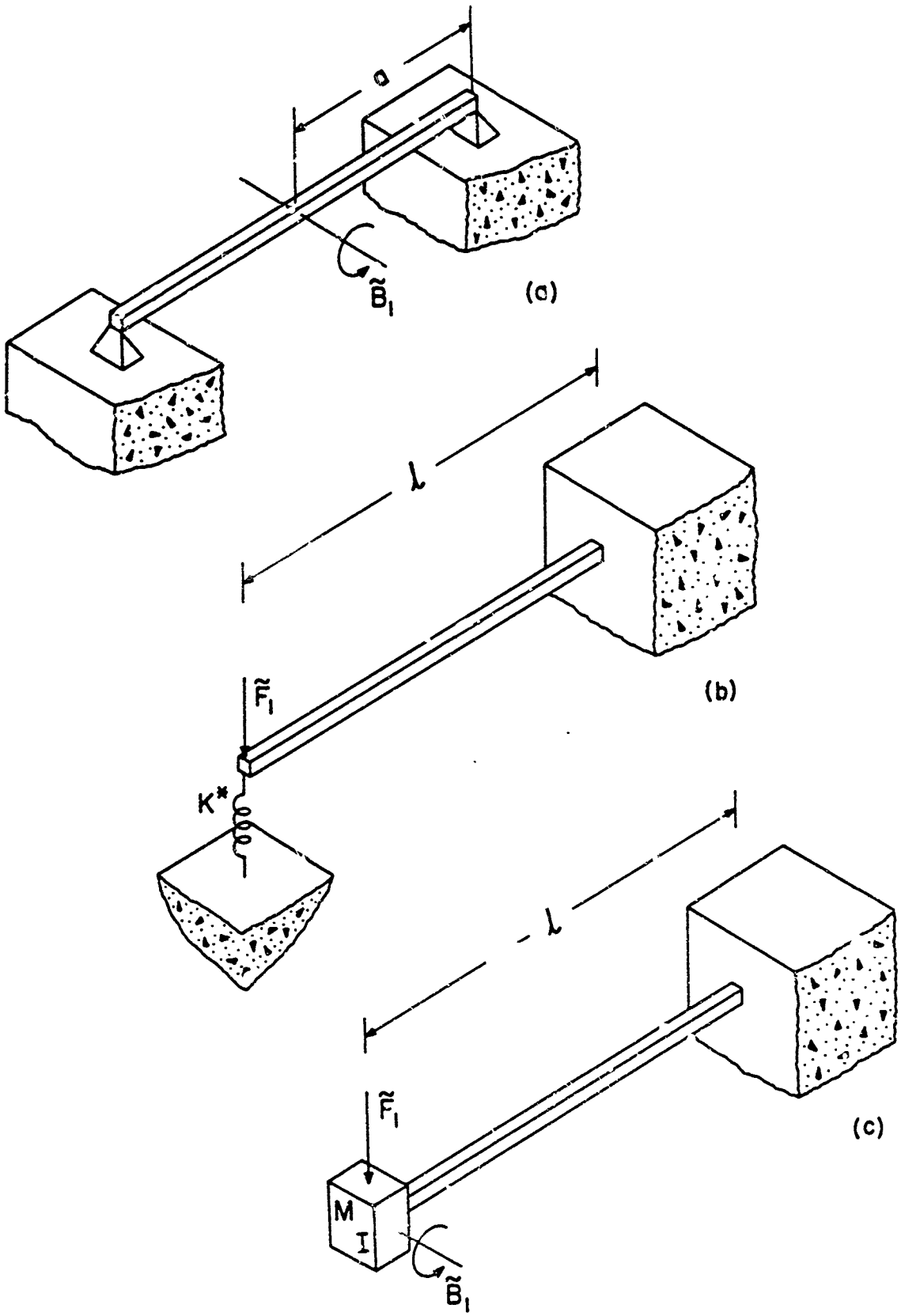

FIG.16

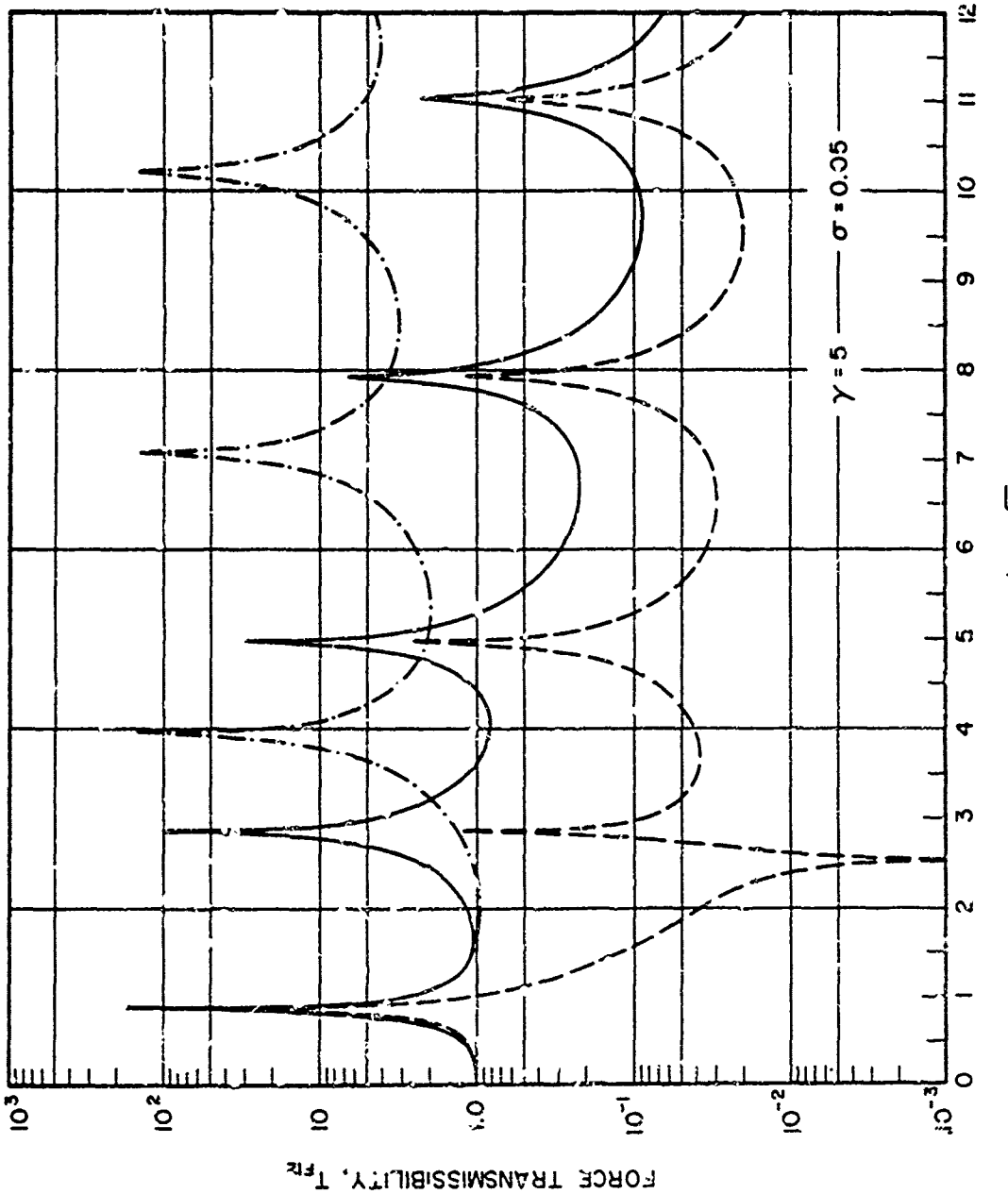
FORCE TRANSMISSIBILITY, T_{FR}
10^{3}
10^{2}
10
1.0
10^{-1}
10^{-2}
10^{-3}
0
1
2
3
4
5
6
7
8
9
10
11
12
$\gamma = 5$ —— $\sigma = 0.05$
$\Omega \propto \omega$

FIG.17

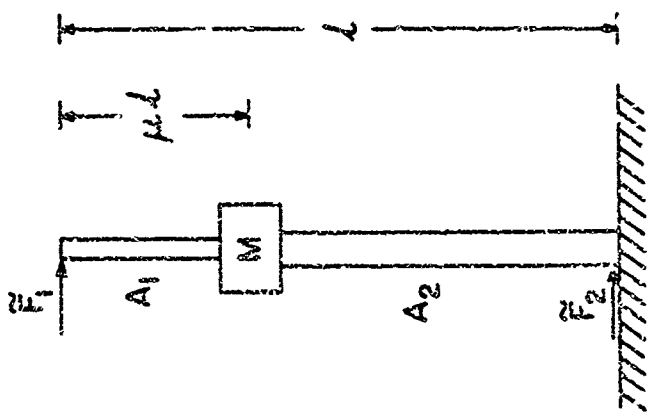

FIG.18

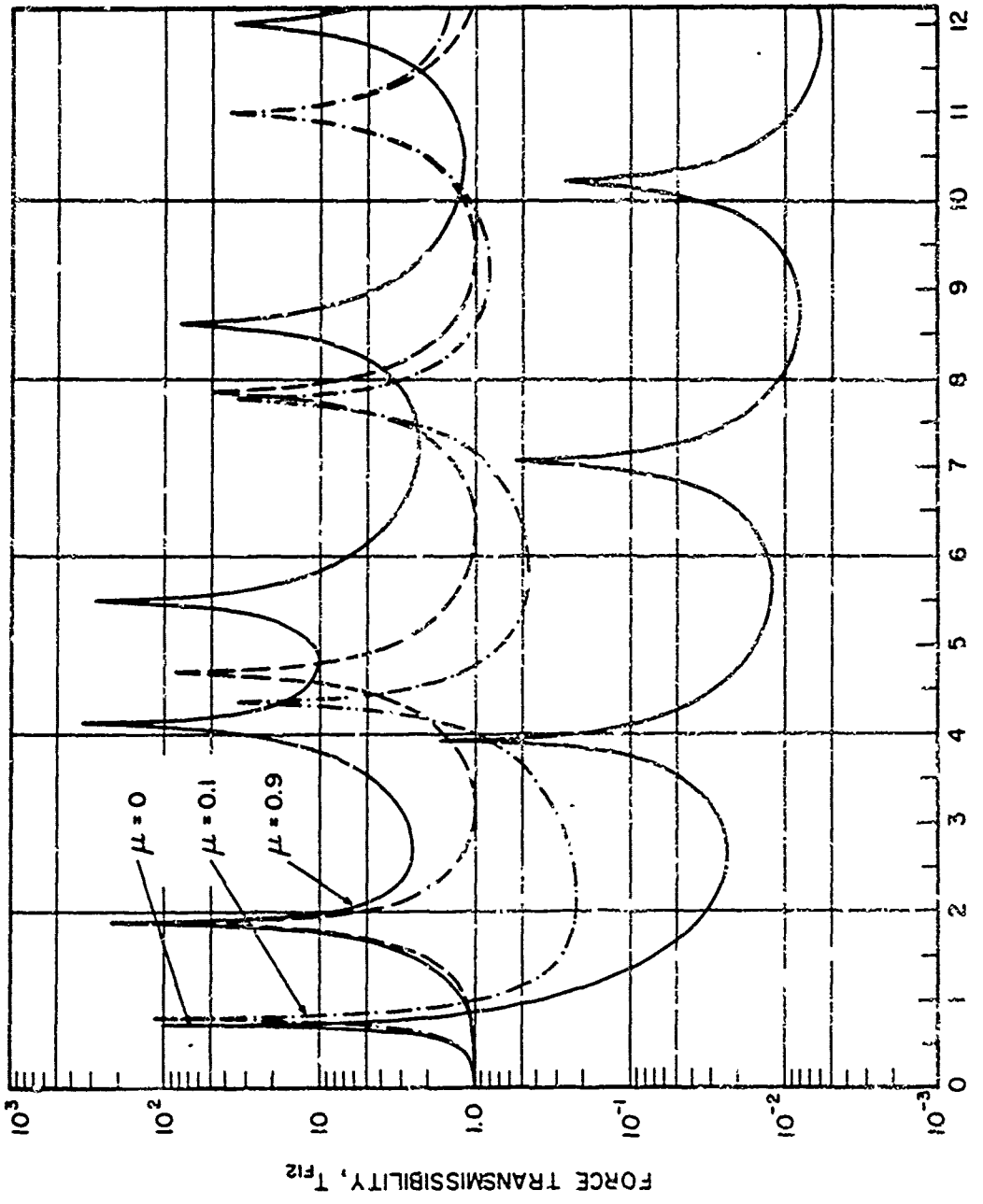
FORCE TRANSMISSIBILITY, T_{Fi2}
10^3
10^2
10
1.0
10^{-1}
10^{-2}
10^{-3}
0
1
2
3
4
5
6
7
8
9
10
11
12
$\eta \propto \gamma\eta$
$\mu = 0$
$\mu = 0.1$
$\mu = 0.9$

FIG.19

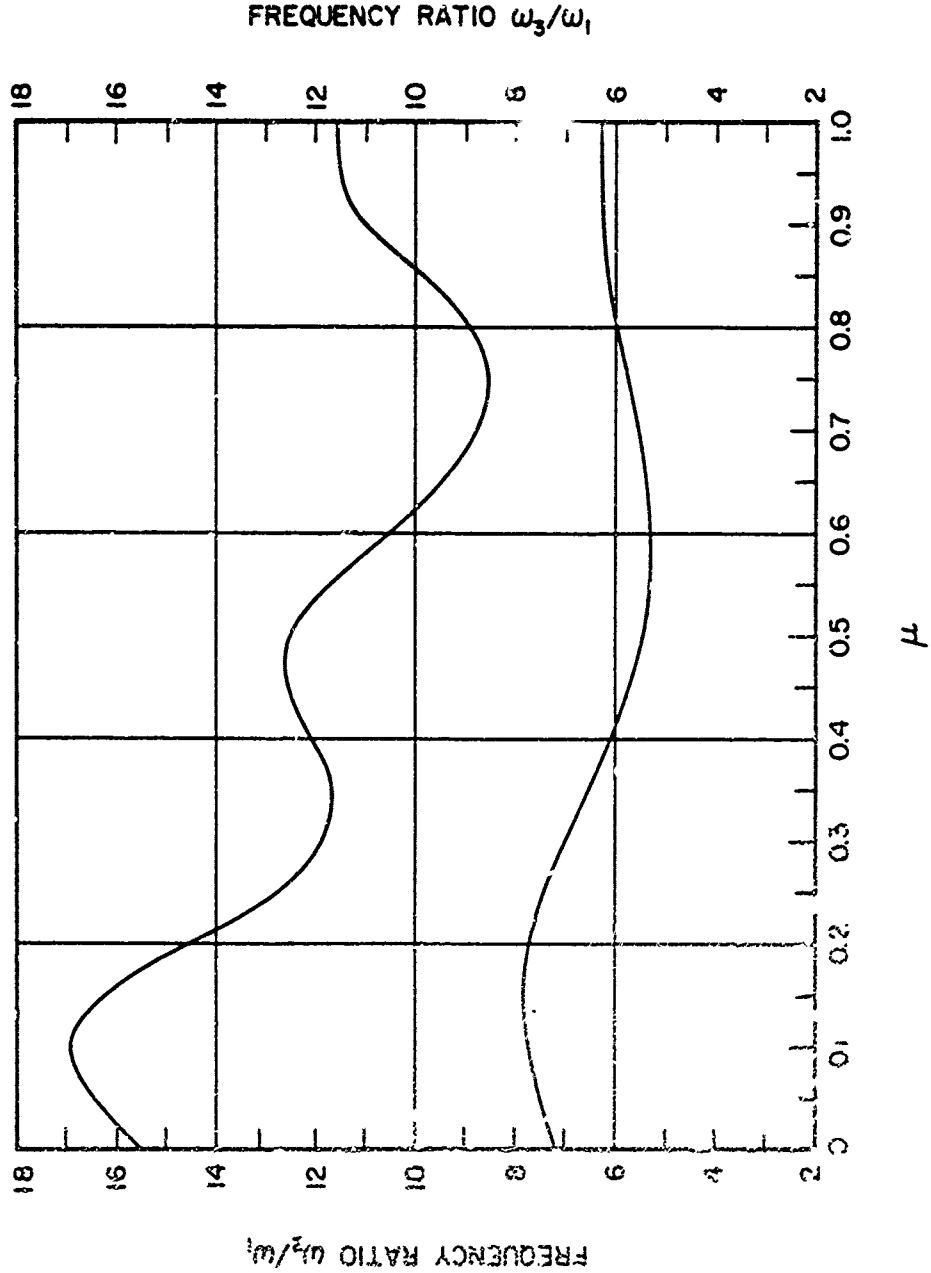
FREQUENCY RATIO ω_3/ω_1
FREQUENCY RATIO ω_2/ω_1
μ
0
0.1
0.2
0.3
0.4
0.5
0.6
0.7
0.8
0.9
1.0
2
4
6
8
10
12
14
16
18

FIG. 20

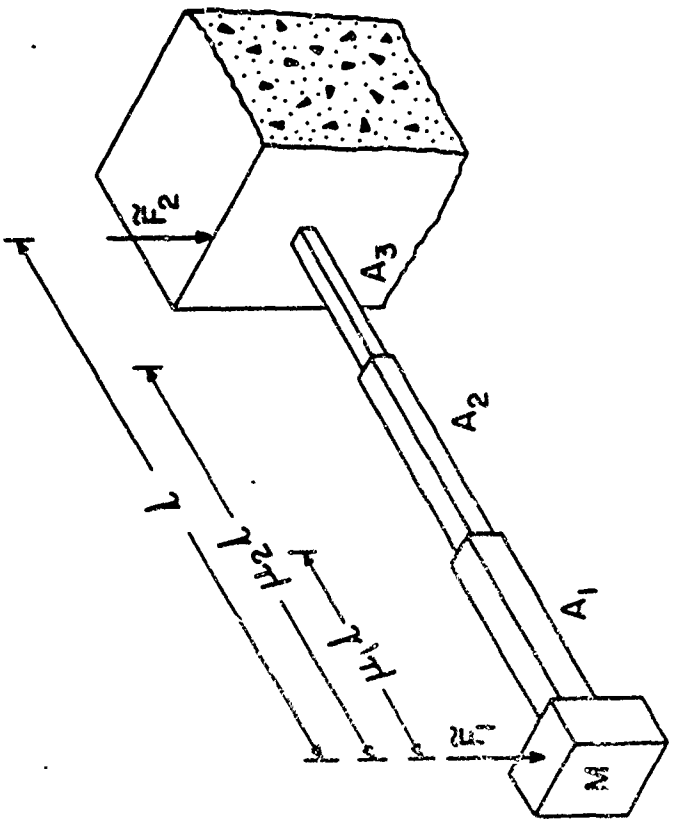

FIG. 21

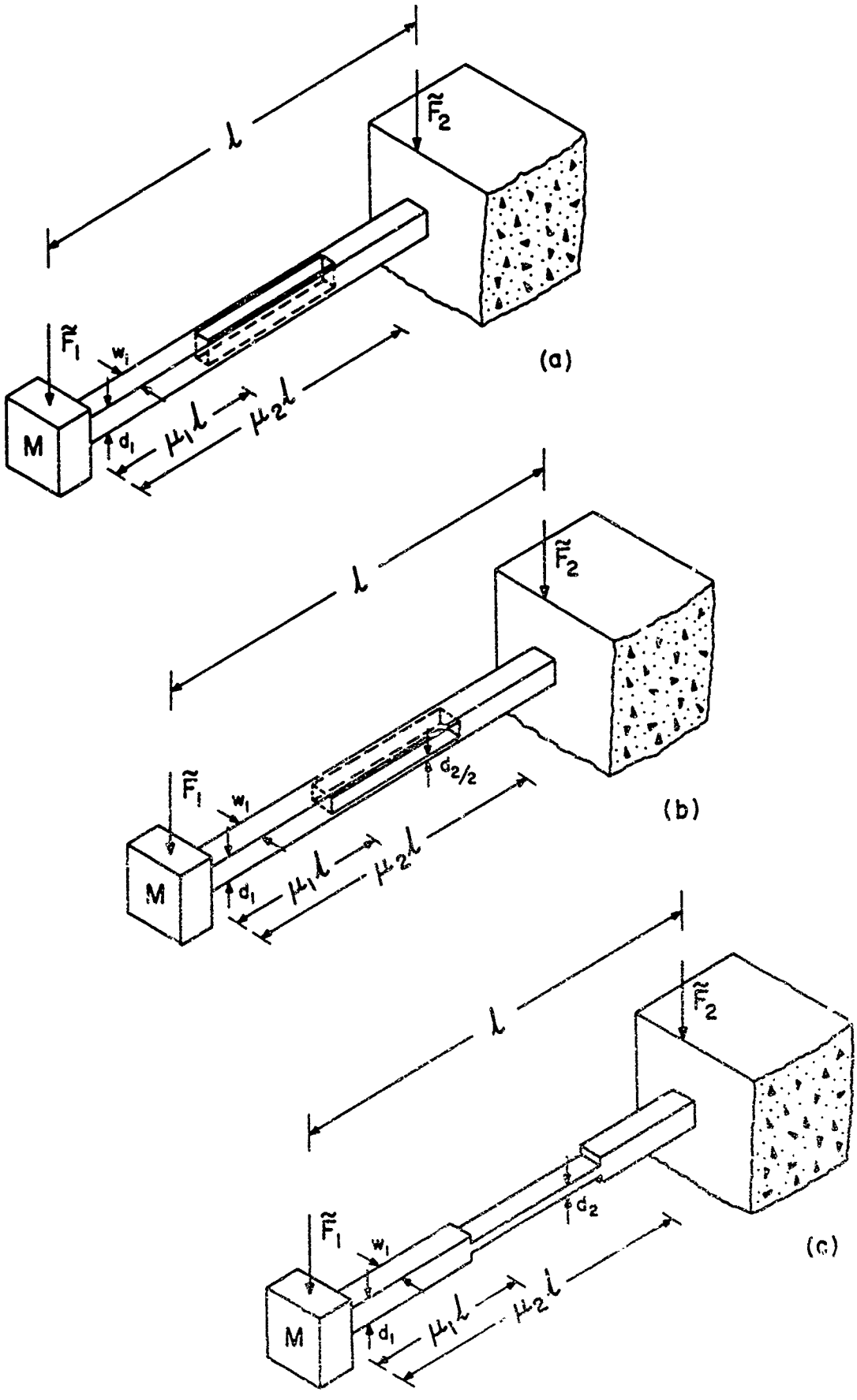

FIG. 22

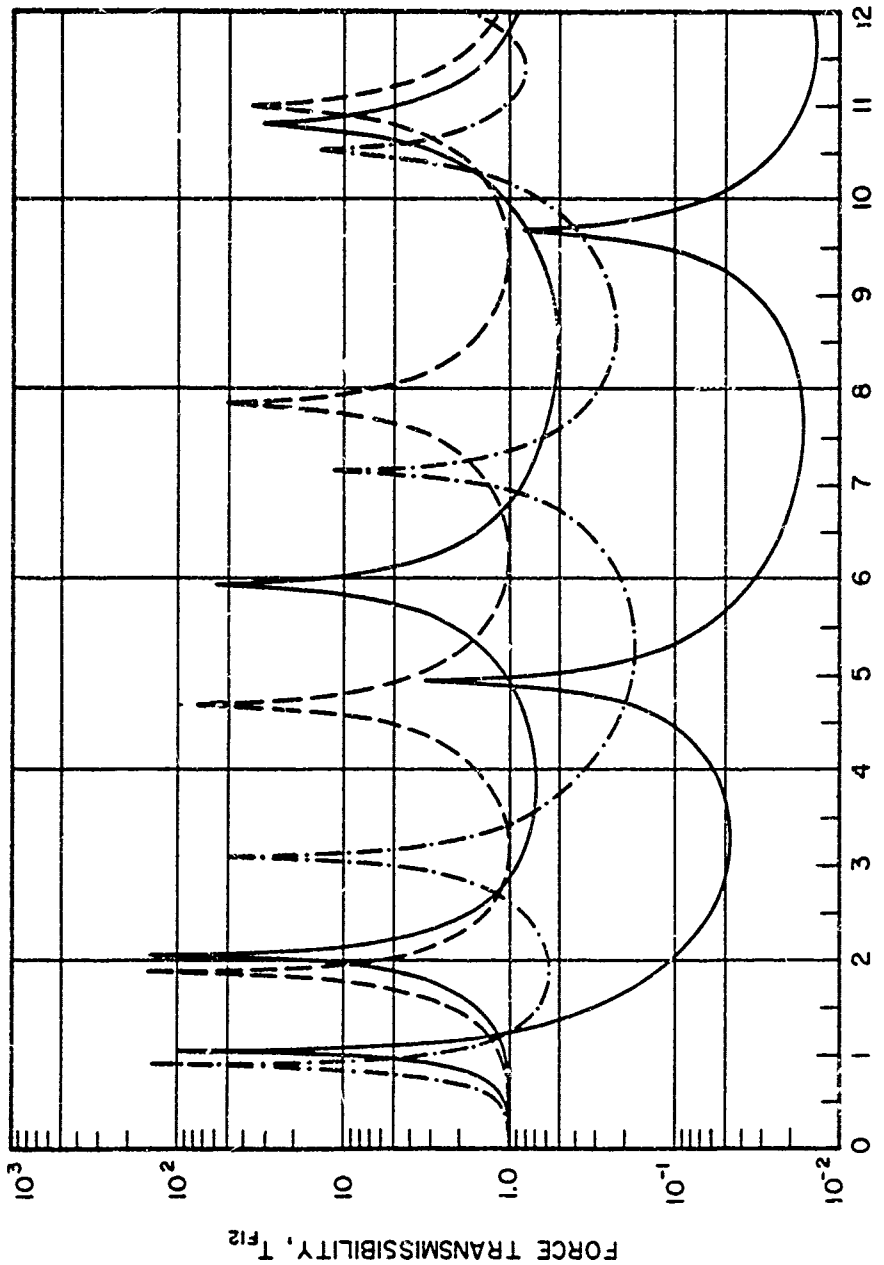
FORCE TRANSMISSIBILITY, T_{Fi2}
10^{3}
10^{2}
10
1.0
10^{-1}
10^{-2}
0
1
2
3
4
5
6
7
8
9
10
11
12
$n_u \propto \sqrt{\omega}$

FIG. 23